AD-778 204

SMALL ANTENNAS FOR NOSE TIP APPLICATIONS

E. H. Newman, et al

Ohio State University

Prepared for:

Harry Diamond Laboratories

April 1974

UNCLASSIFIED

SECURITY CLASSIFICATION OF THIS PAGE *(When Data Entered)*

REPORT DOCUMENTATION PAGE

READ INSTRUCTIONS BEFORE COMPLETING FORM

1. REPORT NUMBER: HDL-TR-041-3	2. GOVT ACCESSION NO.
3. RECIPIENT'S CATALOG NUMBER: AD 778204	
4. TITLE *(and Subtitle)*: SMALL ANTENNAS FOR NOSE TIP APPLICATIONS	5. TYPE OF REPORT & PERIOD COVERED: Final, June 1 - December 31, 1973
	6. PERFORMING ORG. REPORT NUMBER: ESL 3281-5
7. AUTHOR(s): E.H. Newman, J.H. Richmond, G. Chan, C.H. Walter	8. CONTRACT OR GRANT NUMBER(s): DAAG-39-72-C-0041
9. PERFORMING ORGANIZATION NAME AND ADDRESS: The Ohio State University ElectroScience Laboratory, Department of Electrical Engineering, Columbus, Ohio 43212	10. PROGRAM ELEMENT, PROJECT, TASK AREA & WORK UNIT NUMBERS: HDL Project 117215, AMCMS Code 5917.22.70409
11. CONTROLLING OFFICE NAME AND ADDRESS: U.S. Army Materiel Command, Harry Diamond Laboratories, Washington, D.C. 20438	12. REPORT DATE: April 1974
	13. NUMBER OF PAGES: 51
14. MONITORING AGENCY NAME & ADDRESS *(if different from Controlling Office)*	15. SECURITY CLASS. *(of this report)*: Unclassified
	15a. DECLASSIFICATION/DOWNGRADING SCHEDULE

16. DISTRIBUTION STATEMENT *(of this Report)*

Approved for public release; distribution unlimited.

17. DISTRIBUTION STATEMENT *(of the abstract entered in Block 20, if different from Report)*

18. SUPPLEMENTARY NOTES

19. KEY WORDS *(Continue on reverse side if necessary and identify by block number)*

Small Antennas	Efficiency	Modal Analysis	Design Data
Loops	Bandwidth	Moment Method	Dielectric
Dipoles	Impedance	Superconducting	Microstrip Antennas
Gain	Patterns	Active Antennas	Printed Circuit Antennas

20. ABSTRACT *(Continue on reverse side if necessary and identify by block number)*

This report summarizes the work on Contract Number DAAG-39-72-C-0041 for the period June 1, 1973 through December 31, 1973. Previous work on the characteristics of electrically small antennas, antennas in the tip region of a conical projectile, and antennas in or on a conical projectile is briefly reviewed. Using computer modelling new design data for antennas in the tip region of a conical projectile in the frequency range 500 to 1100 MHz is presented. A loop-dipole combination is used to obtain a cardioid type pattern in the forward hemisphere.

DD FORM 1 JAN 73 1473 EDITION OF 1 NOV 65 IS OBSOLETE

UNCLASSIFIED

SECURITY CLASSIFICATION OF THIS PAGE *(When Data Entered)*

HDL Proj 117215
AMCMS Code: 5917.22.70409

HDL-TR-041-3

SMALL ANTENNAS FOR NOSE TIP APPLICATIONS

April 1974

by
E.H. Newman, J.H. Richmond, G. K. Chan, and C.H. Walter

Prepared by:

The Ohio State University ElectroScience Laboratory
Department of Electrical Engineering
Columbus, Ohio 43212

Final Report
Under Contract Number
DAAG-39-72-C-0041
Modification P00001
Exhibit 00024A

U.S. Army Materiel Command
HARRY DIAMOND LABORATORIES
Washington, D.C. 20438

ABSTRACT

This report summarizes the work on Contract Number DAAG-39-72-C-0041 for the period June 1, 1973 through December 31, 1973. Previous work on the characteristics of electrically small antennas, antennas in the tip region of a conical projectile, and antennas in or on a conical projectile is briefly reviewed. Using computer modelling new design data for antennas in the tip region of a conical projectile in the frequency range 500 to 1100 Mhz are presented. A loop-dipole combination is used to obtain a cardioid type pattern in the forward hemisphere.

CONTENTS

I. INTRODUCTION

This report summarizes the work on Contract Number DAAG-39-72-C-0041 for the period June 1, 1973 through December 31, 1973.

The general objective of this program was to develop a numerical method involving computer modelling for analyzing and optimizing a small antenna of arbitrary configuration at the tip of a missile or projectile. Specific antenna configurations to be considered included transverse loops, edgewise loops and loop-dipole combinations, the latter to be used to generate cardioid-type patterns in the forward hemisphere.

Section II of this report summarizes the numerical methods that have been developed and employed on this program. Section III summarizes the scope of the design data that were presented in a previous report and presents all data subsequently developed on this program. Section IV presents conclusions and recommendations.

II. ANALYSIS TECHNIQUES

In the next section the patterns and impedance of several antennas located in the tip region of a conical projectile are presented. These calculations were made using the moment method or current distribution analysis. While a more complete description of the theory and computer programs is available,[1-6] a brief description of the method of moments will now be presented.

---

[1]R. F. Harrington, "Field Computation by Moment Methods," Macmillan, 1968.

[2]J. H. Richmond, "Radiation and Scattering by Thin-Wire Structures in the Complex Frequency Domain," Report 2902-10, July 1973, The Ohio State University ElectroScience Laboratory, Department of Electrical Engineering; prepared under Grant No. NGL 36-008-138 for National Aeronautics and Space Administration.

[3]"Computer Techniques for Electromagnetics," vol. 7, edited by R. Mittra, Pergamon Press, 1973, Chapter 2.

[4]J. H. Richmond, "Computer Program for Thin-Wire Structures in a Homogeneous Conducting Medium," Report 2902-12, August 1973, The Ohio State University ElectroScience Laboratory, Department of Electrical Engineering; prepared under Grant No. NGL 36-008-138 for National Aeronautics and Space Administration.

[5]J. H. Richmond, "Computer Analysis of Three-Dimensional Wire Antennas," Report 2708-4, December 1969, The Ohio State University ElectroScience Laboratory, Department of Electrical Engineering; prepared under Contract DAAD05-69-0031 for Aberdeen Proving Ground.

[6]C. H. Walter and E. H. Newman, "Electrically Small Antennas," Report 3281-3, February 1974, The Ohio State University ElectroScience Laboratory, Department of Electrical Engineering; prepared under Contract DAAG 39-72-C-0041 for Department of the Army, Harry Diamond Laboratories.

Current Distribution Analysis by Moment Method

The current distribution analysis starts with a physical structure and, for a given excitation point or points, either assumes a current distribution from which near and far fields and impedance may be obtained or, preferably, determines the current distribution that satisfies Maxwell's equations and the boundary conditions and then finds the fields and impedance. Until the advent of the high speed digital computer, the most common procedure was to assume a reasonable current distribution or use an approximate analysis, e.g., a transmission line representation, to get an approximate current distribution. Many useful results have been and are being obtained in this manner. However, computer analysis techniques are advancing very rapidly and extremely accurate results can be obtained now for quite complex radiating structures. The following paragraphs outline the basic technique which is called the moment method.

At frequencies where the maximum dimension of the antenna and its support structure are no more than a couple of wavelengths, the antenna and its support structure can often be conveniently approximated by a wire grid model. Such a wire grid structure can be analyzed by the "moment method" which reduces the functional electromagnetic field equations to a set of linear equations that can be handled in a straightforward fashion using well known matrix manipulations on a digital computer. The problem is first formulated in terms of an integral equation with an inhomogeneous source term. Two widely used forms for the integral equation are Pocklington's equation (Ref. 3)

$$(1) \qquad \int_{-L/2}^{L/2} I(z') \left[\frac{\partial^2 G(z,z')}{\partial z^2} + k^2 G(z,z') \right] dz' = -j\omega\varepsilon E_z^i(z)$$

and Hallen's equation (Ref. 3)

$$(2) \qquad \int_{-L/2}^{L/2} I(z')\, G(z,z')\, dz' = \frac{-j}{\eta} \left(C_1 \cos k z + C_2 \sin |k| z \right)$$

where both equations are written for a perfectly conducting dipole of length L along the z axis and with current distribution I(z').

The various quantities in the above equations are defined as

$$G(z,z') = \frac{e^{-jkr}}{4\pi r}$$

$k = 2\pi/\lambda$

η = intrinsic impedance of space

$E_z^i(z)$ = incident field from the source

$C_2 = V_T/2$

V_T = terminal voltage of the antenna

and C_1 is evaluated from the conditions that the current goes to zero at the ends of the antenna.

Either of these equations may be used to solve for the current distribution of an arbitrary wire antenna. However, Pocklington's form is, in a sense, more general since the field E_z^i may be produced by an arbitrary source. Hallen's integral equation uses a delta-gap generator and does not have the flexibility of using different sources of excitation.

The general approach in the method of moments is to reduce the integral equation to a system of linear algebraic equations. The general procedure is illustrated by considering that the integral equation relating the current and the incident field may be written in operator form as

$$L_{op}(J) = (E^i) \tag{3}$$

where E^i is the known source function and the surface current J is the unknown response to be determined. We assume that for a given source there exists one and only one J. That is, an inverse operator exists such that

$$J = L_{op}^{-1} (E^i). \tag{4}$$

The procedure for obtaining a solution for J is as follows:

1) Expand the unknown current distribution in a series of functions which are called basis functions.

2) Define a set of test or weighting functions and determine a suitable inner product of the basis functions and the weighting functions.

3) Take the inner products and thereby form the matrix equation

4) Solve the matrix equation for the unknown currents.

Once the unknown current distribution has been determined, quantities such as far-field patterns, gain and impedance are easily calculated.

Strip Antennas in a Dielectric Slab

A brief outline of work done on the problem of electrically thin strip antennas in or on an electrically thin dielectric slab will now be presented. A more complete description is given in a separate report.[7]

---

[7]E.H. Newman, "Strip Antennas in or on an Electrically Thin Dielectric Slab," Report 3281-4 (in preparation), The Ohio State University ElectroScience Laboratory, Department of Electrical Engineering; prepared under Contract DAAG 39-72-C-0041 for Department of the Army, Harry Diamond Laboratories.

From the volume equivalence theorem the dielectric slab can be replaced with the ambient medium and an equivalent volume polarization current density

$$\underline{J} = j\omega(\epsilon_2-\epsilon)\,\underline{E} \tag{5}$$

where $\underline{E}$ is the electric field intensity in the slab and ϵ_2 and ϵ are the complex permittivities of the slab and ambient medium, respectively. The problem is then reduced to finding $\underline{E}$. Two approaches to finding $\underline{E}$ have been considered.

The first approach considered the current on the strip antenna and the electric field in the dielectric slab to be independent unknowns. The current on the wire strip antenna is expanded in terms of N_W modes and the electric field in the slab in terms of $3N_D$ modes. Thus (N_W+3N_D) linearly independent equations can be written to solve for the unknown current samples on the wire and electric field samples in the slab. In practice this approach was felt to be the most accurate. However, the size of slab one could handle is limited by the storage capabilities of the available digital computer. For a one wavelength square dielectric slab N_D could be 100 and as many as 50,000 complex numbers would need to be stored.

The second approach considers the current on the strip antenna and the electric field in the dielectric slab to be dependent unknowns. The current on the wire strip antenna is expanded in terms of N_W modes and N_W linearly independent equations can be written to solve for the current. For a simple dipole N_W would typically be 4 and the impedance matrix would consist of only 10 complex numbers. The effects of the dielectric are accounted for through a modification of the impedance matrix. To make these modifications one must be able to approximate the electric field intensity radiated by the N_W expansion modes in the presence of the dielectric slab. Because of the greatly reduced requirement on computer storage, it was decided to pursue this second approach (Ref. 7). While the expressions presented for the fields of the expansion modes were approximate, they had the advantage that they were fast and easy to evaluate on a digital computer. The theory was compared with measurements for strip dipole antennas in and on a thin dielectric slab with very good agreement being obtained even for a slab as much as one-quarter inch thick and frequencies as high as 1000 MHz (Ref. 7).

III. ANTENNAS IN THE TIP OF A PROJECTILE

In a previous report (Ref. 6) the impedance, efficiency, and patterns of several antennas mounted in the tip region of the projectile of Fig. 1 were presented. The frequency range covered was 150 to 500 MHz and the following tip configurations were considered:

1. A 4-1/2 turn helical stub with conical tip.

2. A 4-1/2 turn helical stub without conical tip.

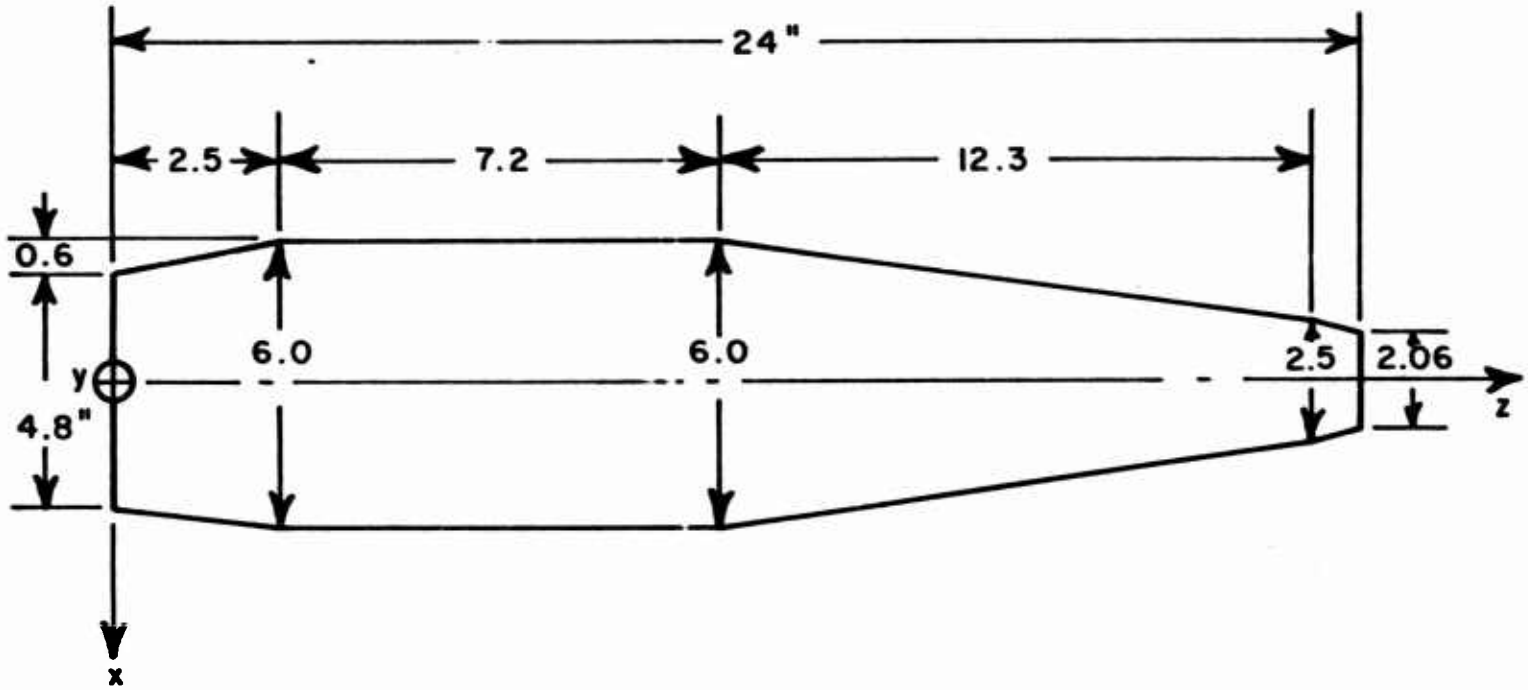

Fig. 1. Outline of the projectile body. A hexagonal cross-section was used in the mathematical model.

3. A triangular loop in the xz plane attached to the top surface of the projectile.

4. A simple vertical stub exciting a gap in the projectile body.

The purpose of this section is to present the patterns and impedance of three different antennas located in the tip region of the projectile. The data presented here will be in the 500 to 1100 MHz range. The calculations were made by modeling the projectile and antenna by a wire-grid structure as before (Ref. 6). The wire-grid model is then analyzed using moment methods and the piecewise-sinusoidal reaction formulation. The details of this approach to modeling antennas are given elsewhere (Refs. 1-6).

The specific tip configurations to be considered are:

1. A vertical triangular loop.
2. A horizontal hexagonal loop.
3. A loop-dipole combination.

For the first two of the above configurations the effects on the impedance of capacitive loading and varying the loop position will be investigated. For the range of values considered the loop position had no significant effect on the patterns, and the loading had no significant effect on the patterns for the vertical loop.

Pattern and Impedance Data

Case 1 - The vertical triangular loop

Figure 2 shows a vertical triangular loop in the tip region of the projectile of Fig. 1. The loop is located in the xz plane a distance ΔZ from the top surface of the projectile, and is fed at its tip. A Smith Chart plot of the impedance of the loop is shown in Fig. 3 for $\Delta Z = 0.25$ and for f = 500, 600, ··· 1100 MHz. The corresponding patterns are shown in Figs. 4 a-g. The polarization is essentially in the θ direction. The patterns are essentially those of the loop in free-space, although the projectile does cause some distortion especially at the higher frequencies.

The effect of placing three capacitors, one in each arm of the loop, is shown in Fig. 5. Here the loop impedance at f = 900 MHz and $\Delta Z = 0.25$ in. is plotted versus the capacitive reactance of each of the capacitors inserted. Both the real and imaginary parts of the loop impedance decrease as the capacitive reactance increases. Extrapolation of the data from Fig. 5 indicates that the loop impedance at resonance (radiation resistance) is about 6 ohms.

Figure 6 shows the impedance of the unloaded loop at f = 900 MHz as a function of ΔZ, the height of the loop above the projectile. As expected, the input impedance is the strongest function of ΔZ when ΔZ is small.

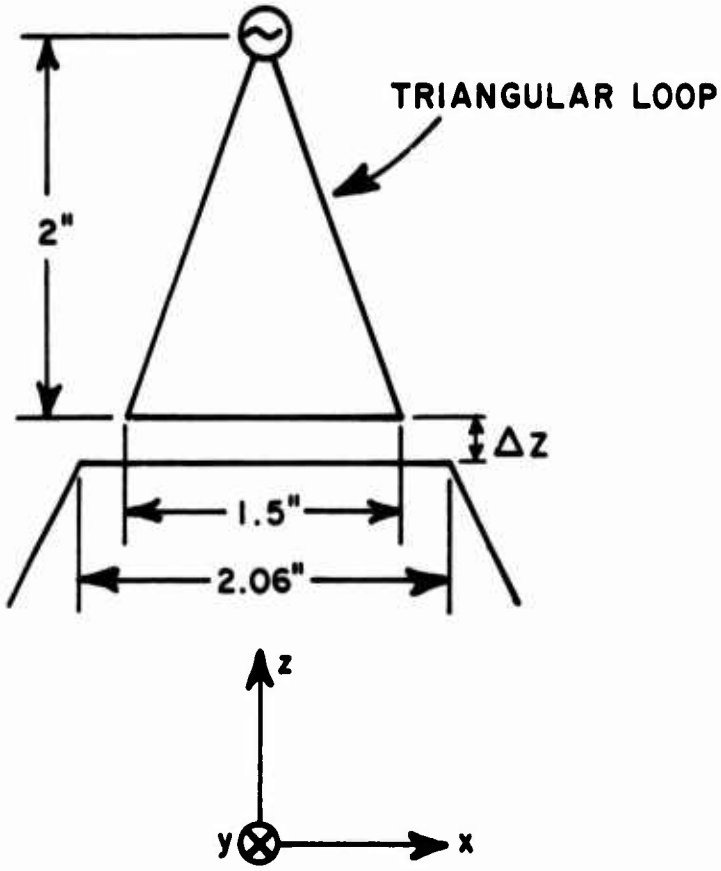

Fig. 2. A vertical triangular loop in the tip region of the projectile shown in Fig. 1.

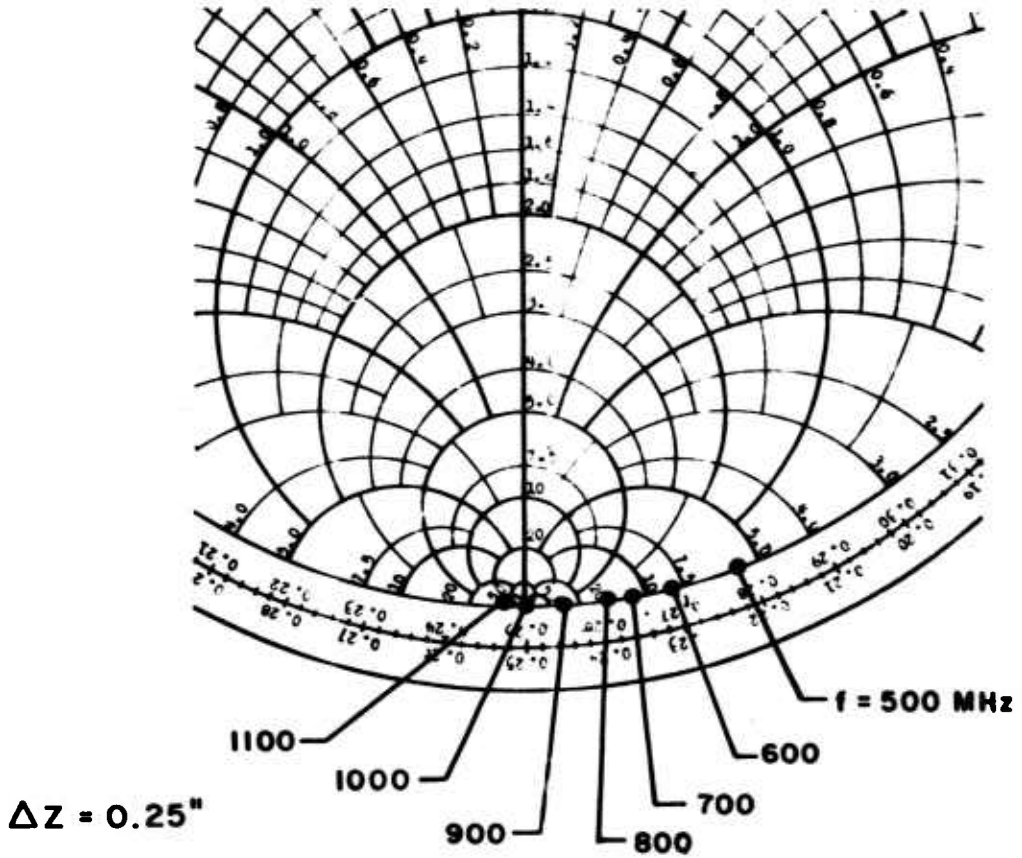

Fig. 3. A Smith Chart plot of the impedance of the antenna of Fig. 2.

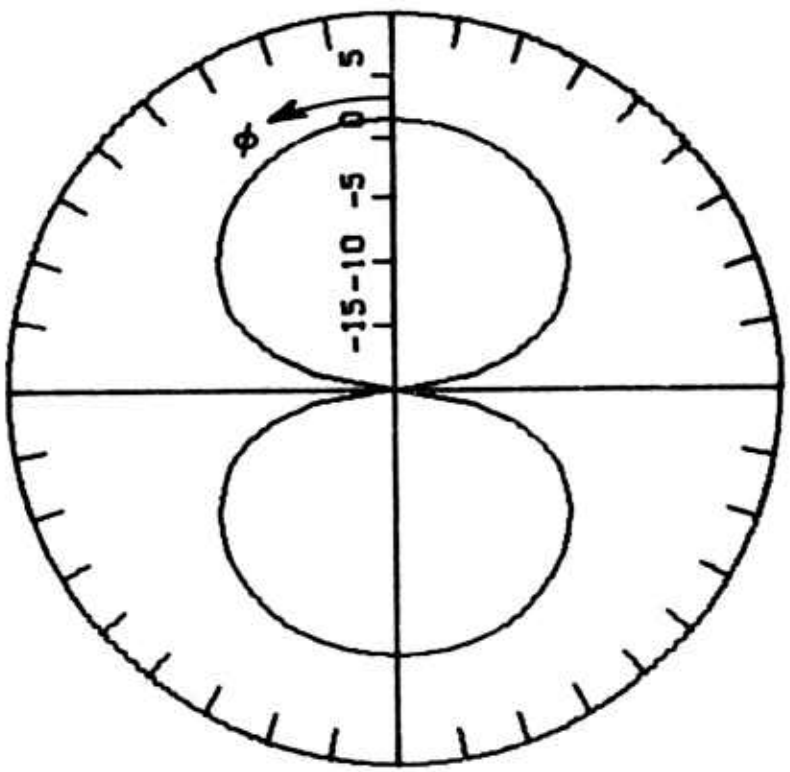

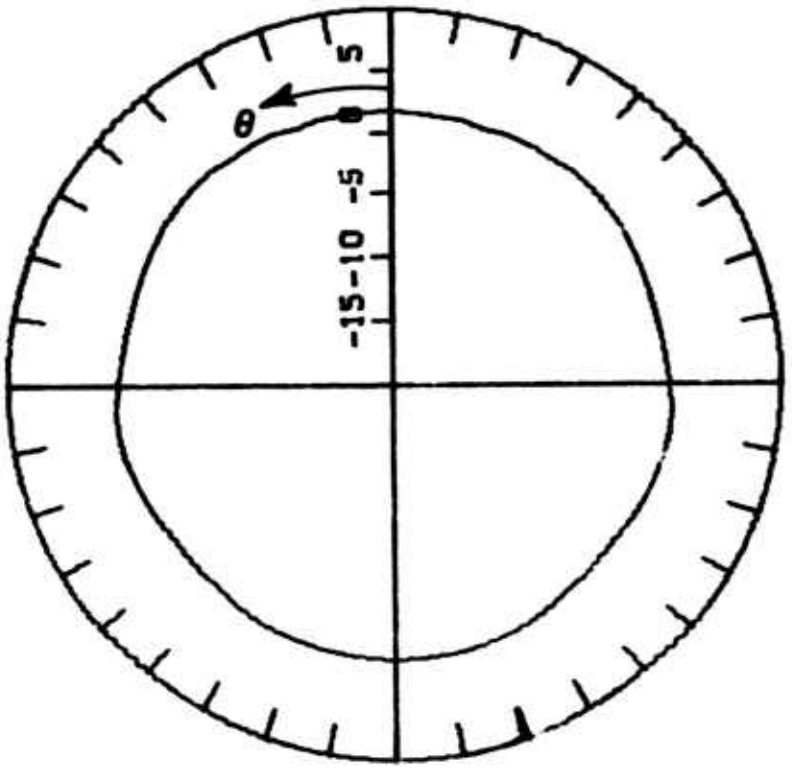

PATTERN IN THE PLANE
THETA = PI/2.

PATTERN IN THE PLANE
PHI = 0.PI.

FREQ. (MHZ) = 500.0
TIP CONFIGURATION 5 DZ = 0.25 IN.

Fig. 4a. $\hat{\theta}$ polarized directivity for the antenna of Fig. 2 at f = 500 MHz.

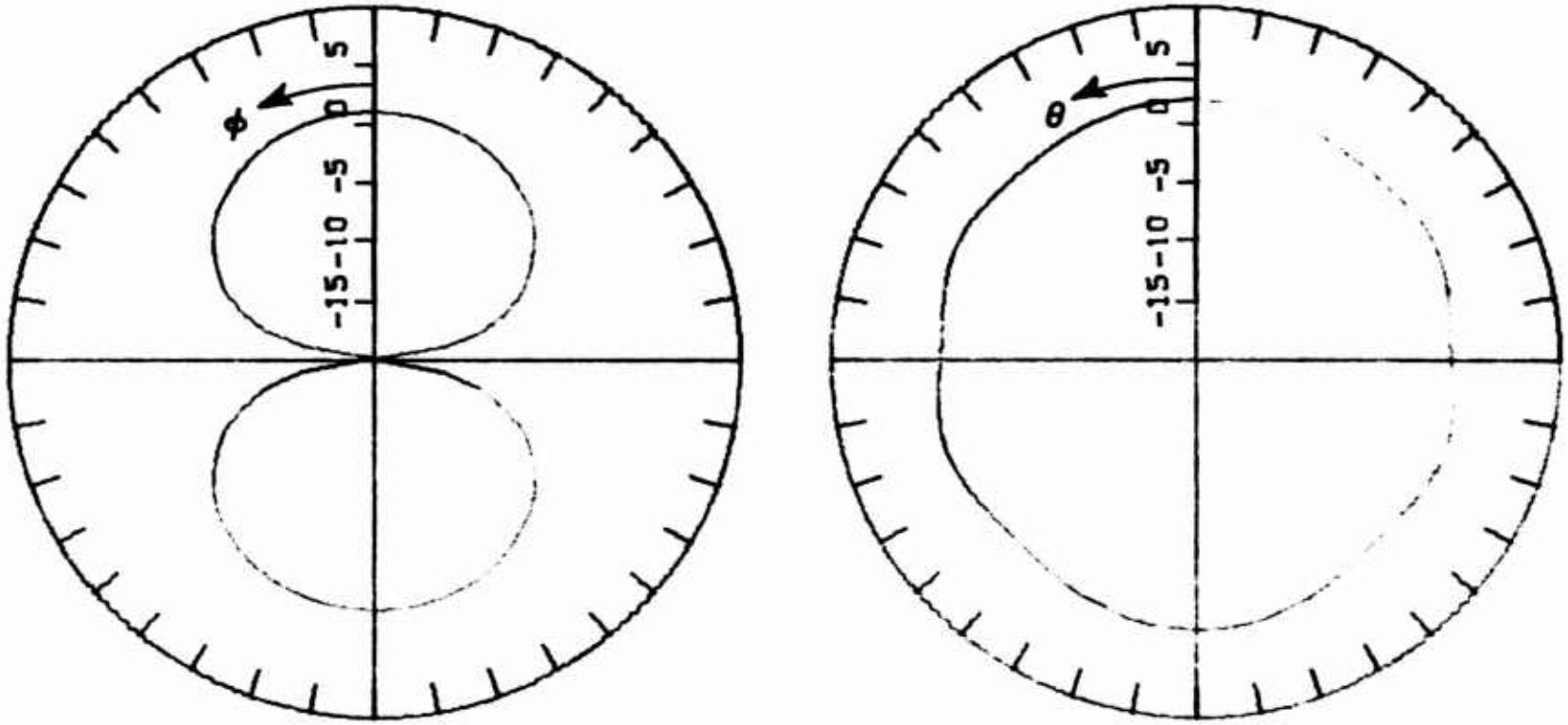

PATTERN IN THE PLANE
THETA = PI/2.

PATTERN IN THE PLANE
PHI = 0.PI.

FREQ. (MHZ) = 600.0
TIP CONFIGURATION 5 DZ = 0.25 IN.

Fig. 4b. $\hat{\theta}$ polarized directivity for the antenna of Fig. 2 at f = 600 MHz.

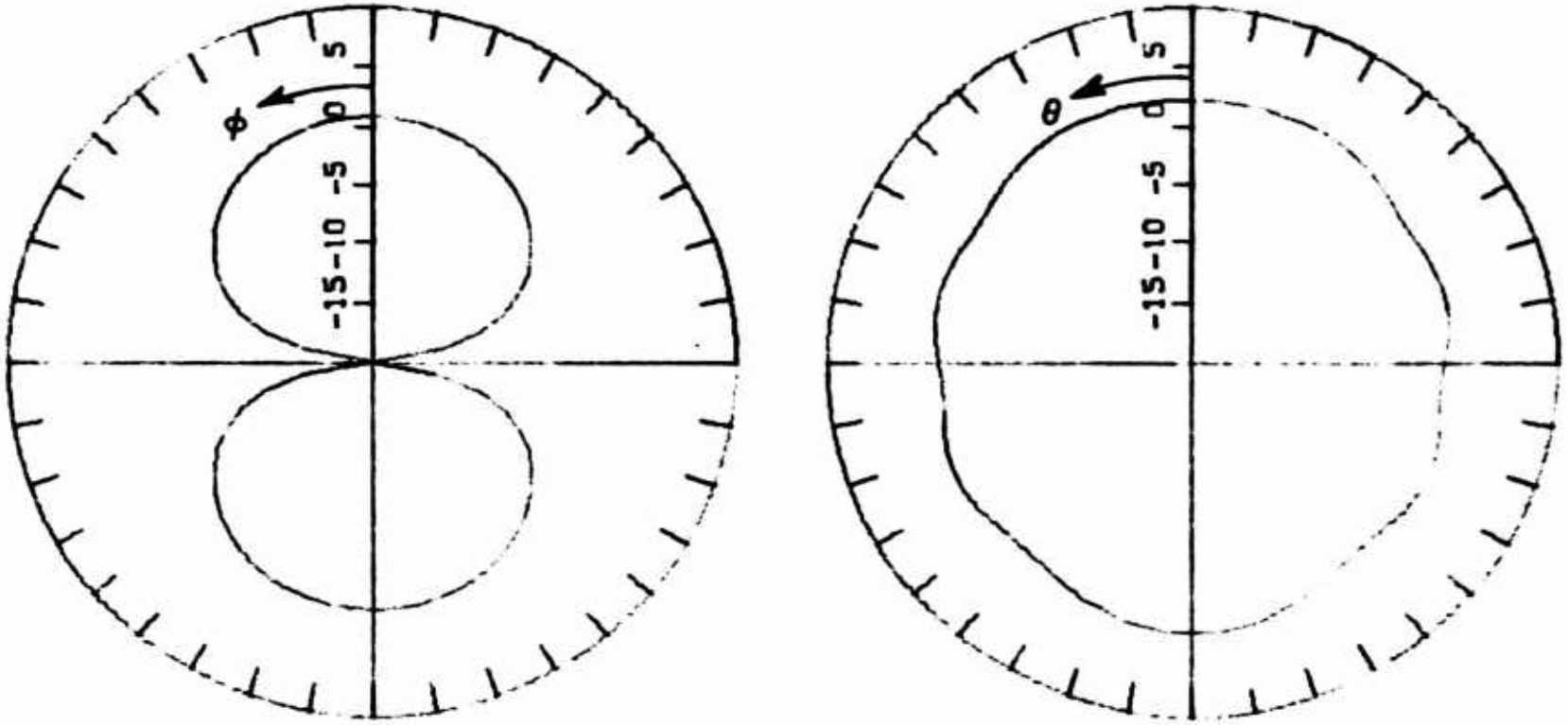

PATTERN IN THE PLANE
THETA = PI/2.

PATTERN IN THE PLANE
PHI = 0.PI.

FREQ. (MHZ) = 700.0
TIP CONFIGURATION 5 DZ = 0.25 IN.

Fig. 4c. $\hat{\theta}$ polarized directivity for the antenna of Fig. 2 at f = 700 MHz.

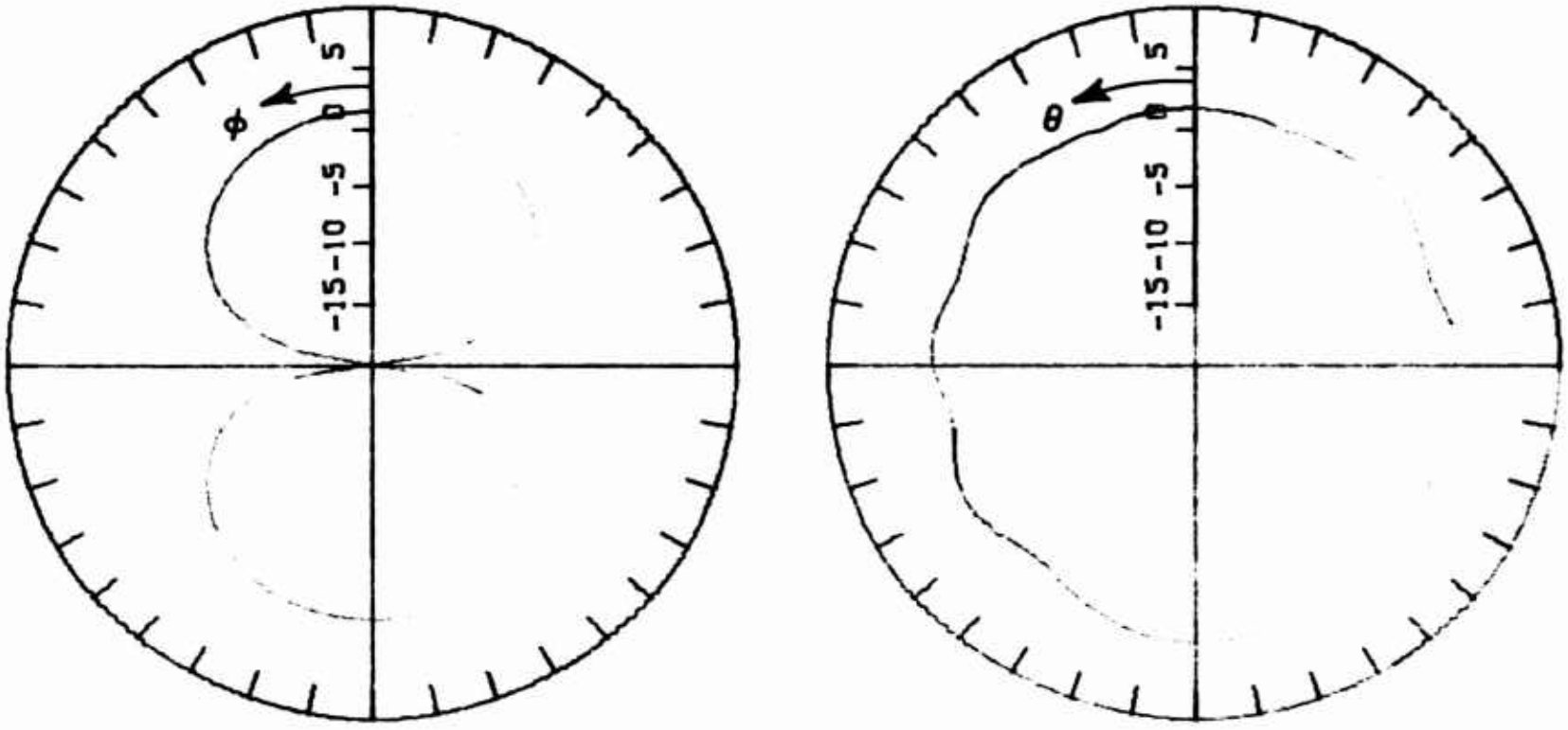

PATTERN IN THE PLANE
THETA = PI/2.

PATTERN IN THE PLANE
PHI = 0.PI.

FREQ. (MHZ) = 800.0
TIP CONFIGURATION 5 DZ = 0.25 IN.

Fig. 4d. $\hat{\theta}$ polarized directivity for the antenna of Fig. 2 at f = 800 MHz.

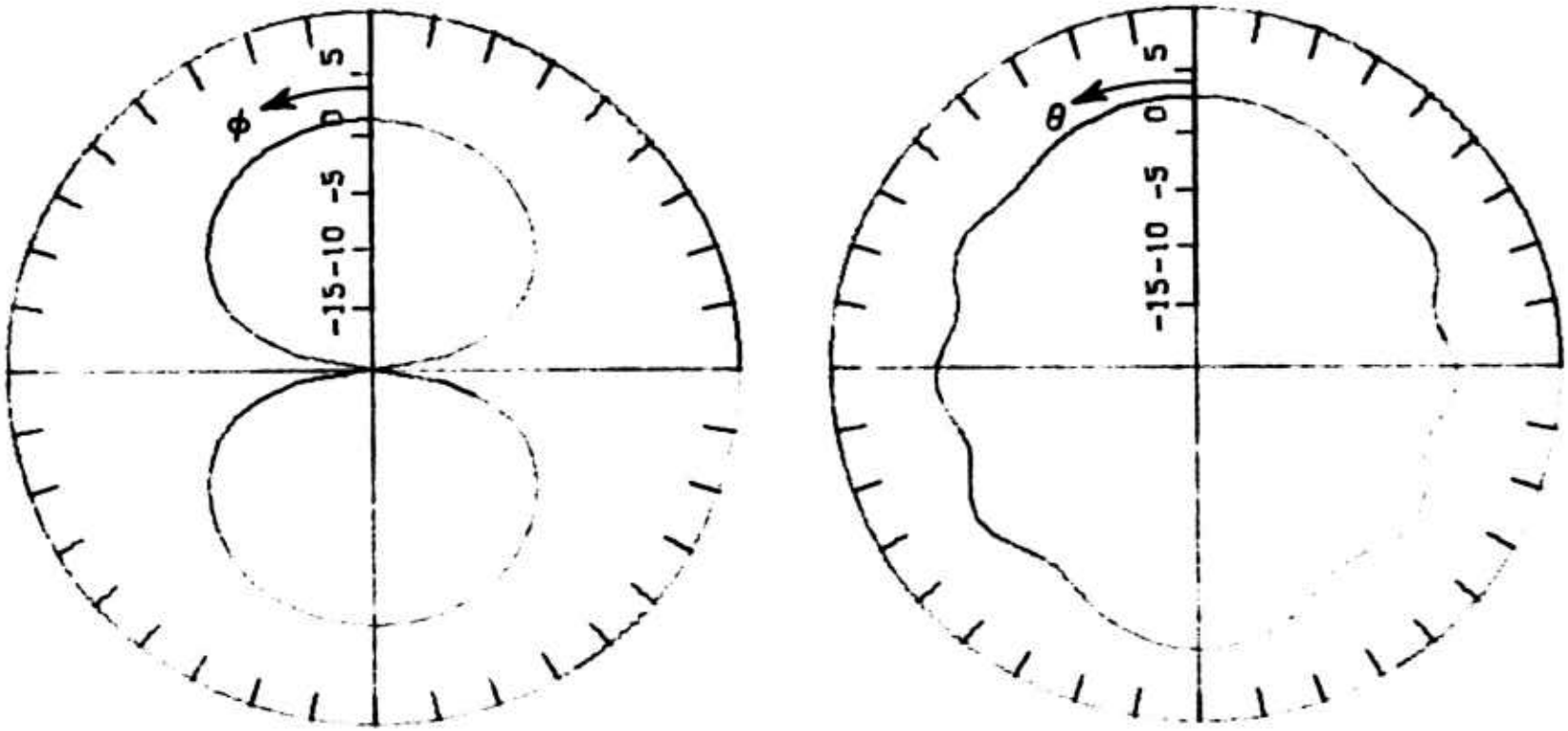

PATTERN IN THE PLANE
THETA = PI/2.

PATTERN IN THE PLANE
PHI = 0.PI.

FREQ. (MHZ) = 900.0
TIP CONFIGURATION 5 DZ = 0.25 IN.

Fig. 4e. $\hat{\theta}$ polarized directivity for the antenna of Fig. 2 at f = 900 MHz.

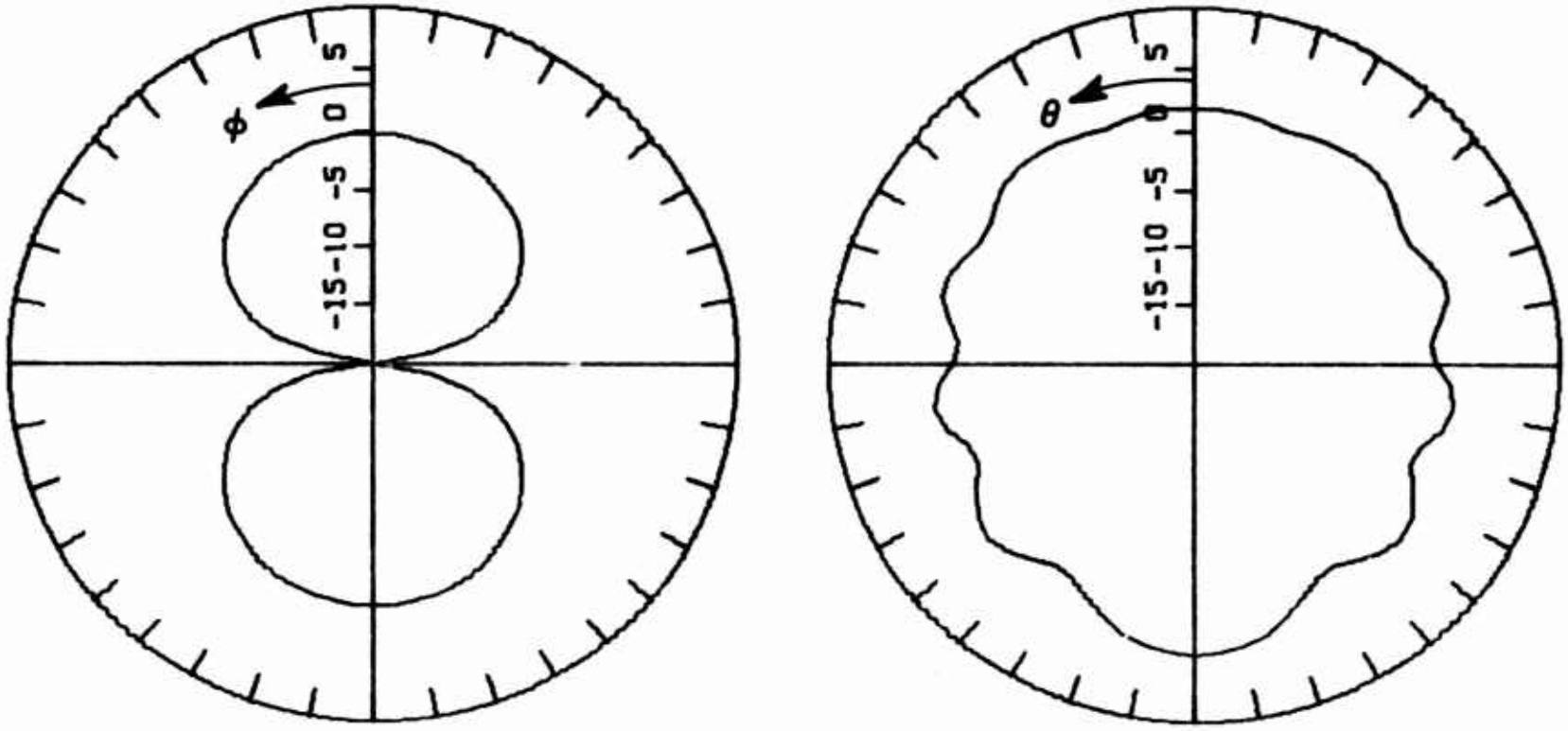

PATTERN IN THE PLANE
THETA = PI/2.

PATTERN IN THE PLANE
PHI = 0.PI.

FREQ. (MHZ) = 1000.0
TIP CONFIGURATION 5 DZ = 0.25 IN.

Fig. 4f. $\hat{\theta}$ polarized directivity for the antenna of Fig. 2 at f = 1000 MHz.

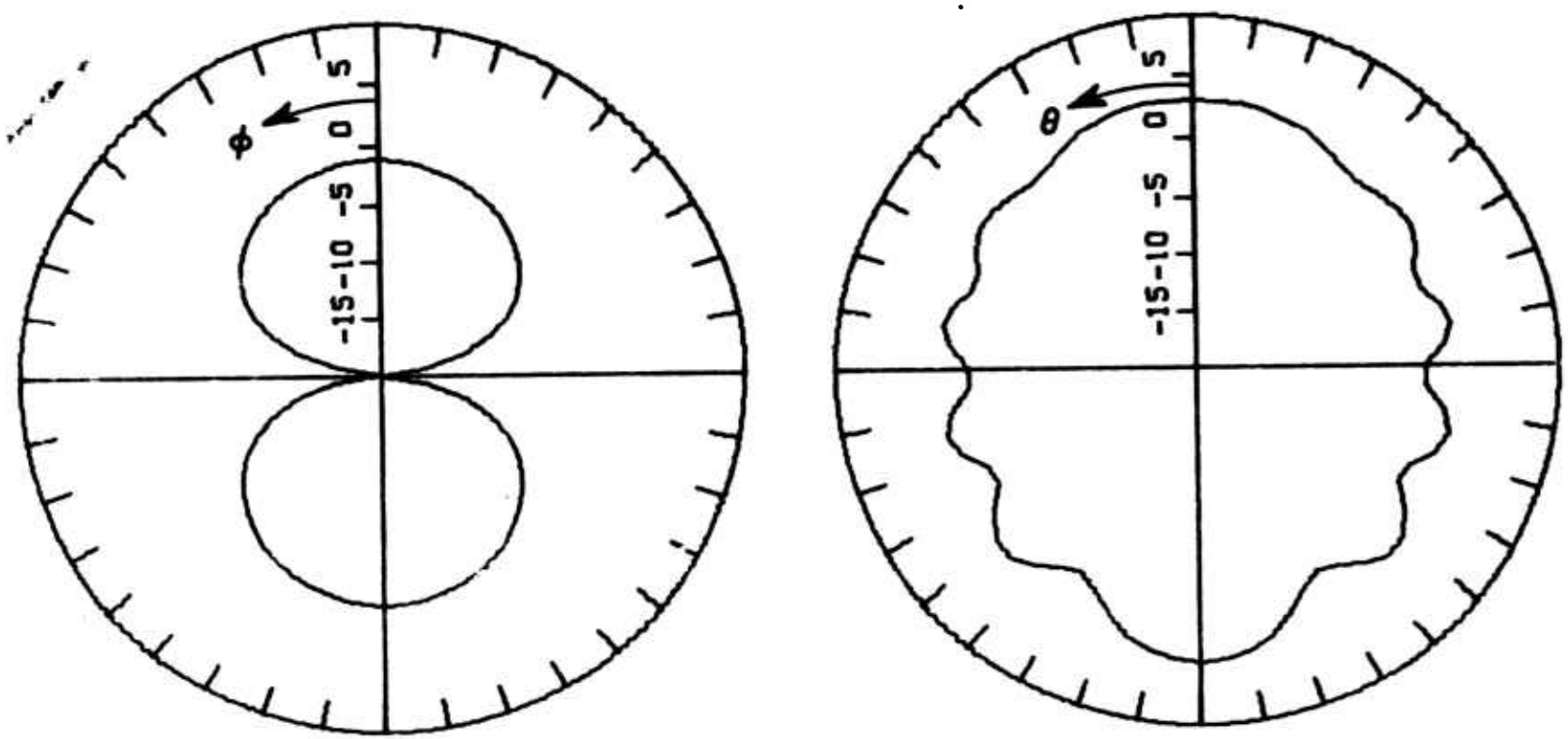

PATTERN IN THE PLANE
THETA = PI/2.

PATTERN IN THE PLANE
PHI = 0.PI.

FREQ. (MHZ) = 1100.0
TIP CONFIGURATION 5 DZ = 0.25 IN.

Fig. 4g. $\hat{\theta}$ polarized directivity for the antenna of Fig. 2 at f = 1100 MHz.

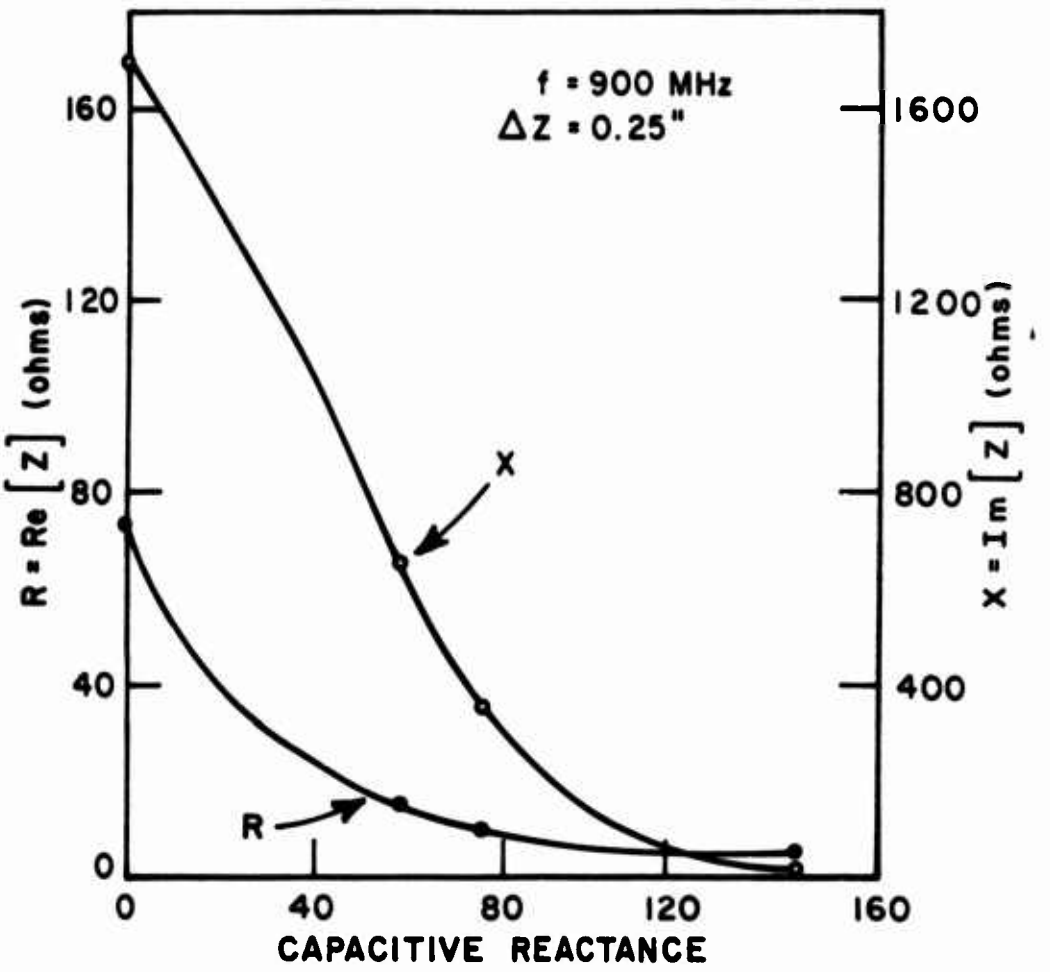

Fig. 5. The impedance of the antenna of Fig. 2 at f = 900 MHz plotted versus the reactance of three capacitors inserted in the triangular loop.

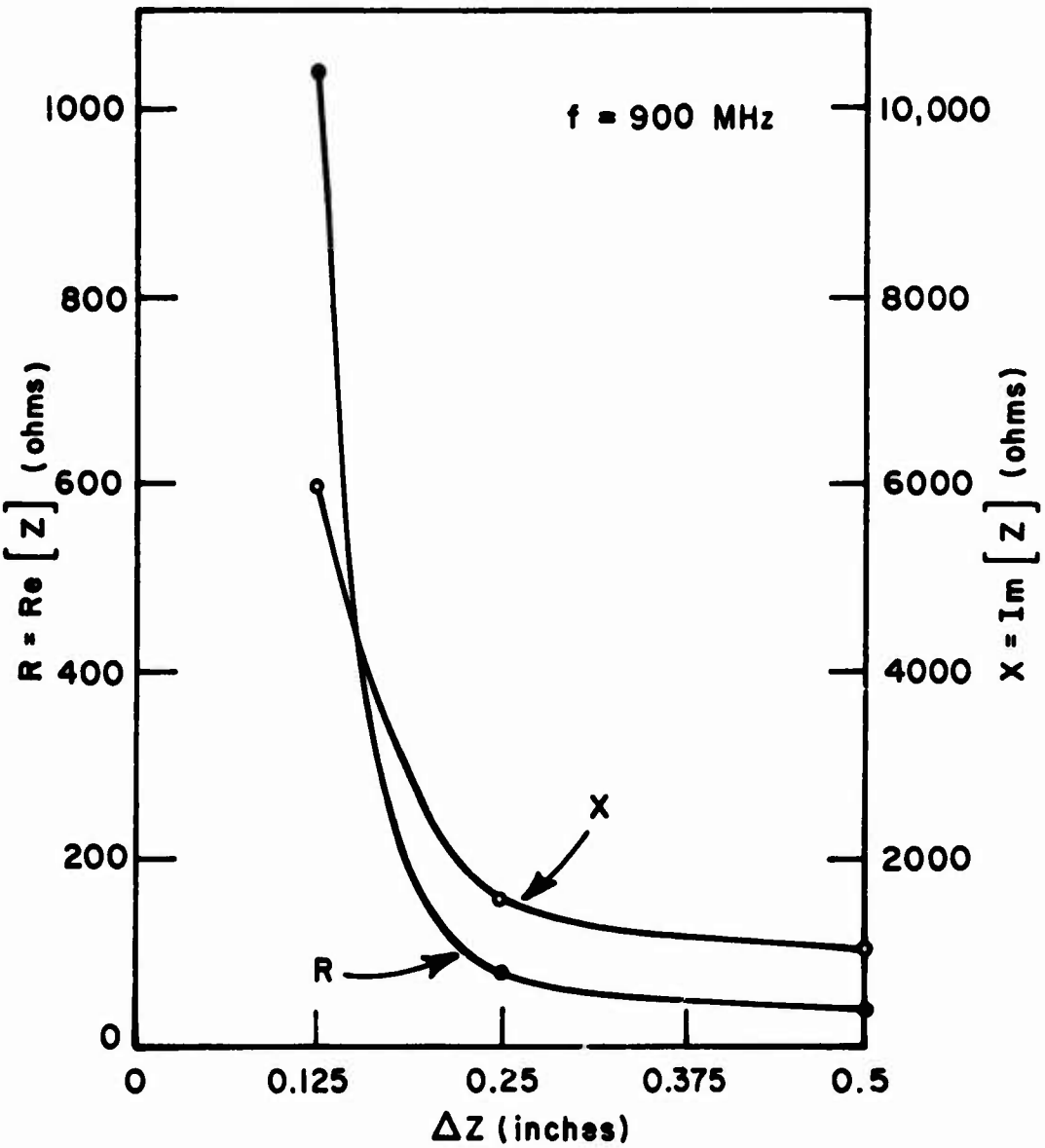

Fig. 6. The impedance of the antenna of Fig. 2 at f = 900 MHz plotted versus ΔZ.

Case 2 - The horizontal hexagonal loop

Figure 7 shows a hexagonal loop located a distance ΔZ above the top surface of the projectile of Fig. 1. The loop is in a plane parallel to the xy plane, and its circumference is the same as that of the triangular loop previously described. A Smith Chart plot of the impedance of the loop is shown in Fig. 8 for $\Delta Z = 0.25$ in. and for f = 500, 600, ... 1100 MHz. The corresponding patterns are shown in Figs. 9 a-g. The polarization is essentially in the $\hat{\phi}$ direction. The pattern in the plane $\theta = \pi/2$ is omnidirectional as one would expect. The projectile does significantly alter the patterns in the plane $\phi = 0,\pi$. Note that the null on the loop axis decreases as the frequency increases. This is mostly due to the fact that the loop current becomes less uniform as the frequency increases, but is partly due to the fact that the loop excites the cone body more at the higher frequencies.

The effect on the loop impedance of inserting three capacitors in the loop at f = 1000 MHz and $\Delta Z = 0.25$ in. is shown in Fig. 10a. Figure 10b shows that the capacitive loading significantly effects the patterns in the plane $\phi = 0,\pi$. The patterns in the plane $\theta = \pi/2$ are not as effected by the loading and are shown in Fig. 10c. The capacitors were inserted at the generator and then every other junction proceeding counterclockwise (viewed from the positive z axis).

The effect of varying the height of the loop above the projectile at f = 1000 MHz is shown in Fig. 11. For the range of ΔZ covered the impedance increased with increasing ΔZ.

Case 3 - The loop-dipole combination

Figure 12 shows a loop-dipole combination in the tip region of the projectile. Both the loop and the dipole are in the xz plane. The dipole is center fed, and the triangular loop is fed at its tip. The distance from the projectile to the dipole and the distance from the dipole to the bottom arm of the loop is denoted by ΔZ. The impedance seen at the dipole terminals with the loop generator short circuited and the impedance seen at the loop terminals with the dipole generator short circuited are shown in Fig. 13.

The purpose for considering the loop-dipole combination was to obtain a cardioid-type pattern in the xz plane with the null at $\theta = 180°$. The cardioid-type pattern can be obtained at a given frequency as follows. First the pattern is generated for the loop fed with a one volt generator and the dipole generator short circuited. Denote the $\hat{\theta}$ polarized electric field at $\theta = 180°$ as E_L ($\theta = 180°$). Similarly, with the dipole fed with a one volt generator and the loop generator short circuited the $\hat{\theta}$ polarized electric field at $\theta = 180°$ is denoted E_D ($\theta = 180°$). If the loop is now fed with a generator of one volt and the dipole with a generator of V_D volts, then using superposition the $\hat{\theta}$ polarized electric field at $\theta = 180°$ for the loop dipole combination will be

$$E_{LD}\ (\theta = 180°) = E_L\ (\theta = 180°) + V_D\ E_D\ (\theta = 180°). \tag{6}$$

The cardioid-type pattern will be obtained if E_{LD} ($\theta = 180°$) = 0 or

(7) $$E_L\ (\theta = 180°) + V_D E_D\ (\theta = 180°) = 0$$

or

(8) $$V_D = -\ E_L\ (\theta = 1800)/E_D\ (\theta = 180°).$$

Note that E_L ($\theta = 180°$) and E_D ($\theta = 180°$) must include both magnitude and phase. Using Eq. (8) at f = 900 MHz it was found $V_D = 5.82 + j8.67$. The patterns for the $\hat{\theta}$ polarization are shown in Figs. 14 a-f for the frequencies f = 600, 700, ... 1100 MHz and $\Delta Z = 0.25$ in. Note that at f = 900 MHz the cardioid-type pattern is obtained. As the frequency departs from 900 MHz the resemblance to the cardioid decreases. The patterns for the $\hat{\phi}$ polarization in the plane $\theta = \pi/2$ are shown in Figs. 15 a-c. In the plane $\phi = 0, \pi$ the $\hat{\phi}$ polarization is negligible.

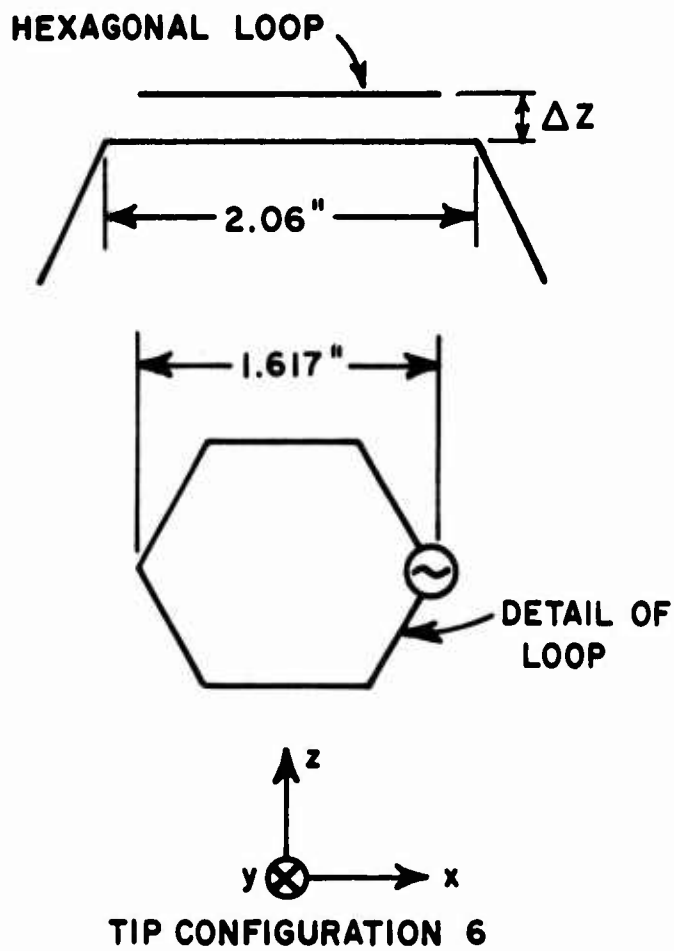

Fig. 7. A horizontal hexagonal loop located in the tip region of the projectile of Fig. 1.

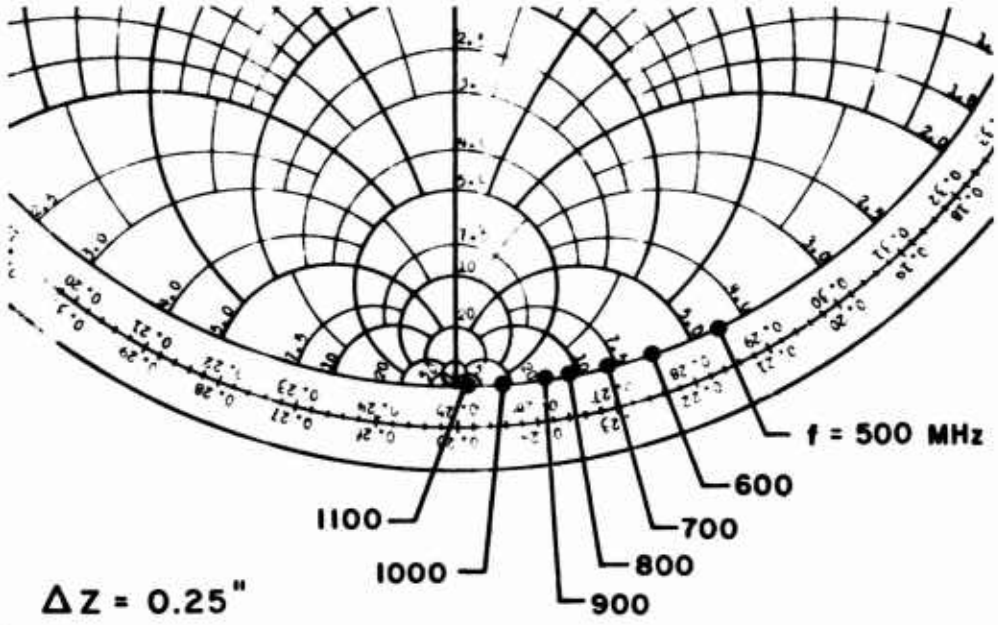

Fig. 8. A Smith Chart plot of the impedance of the antenna of Fig. 7.

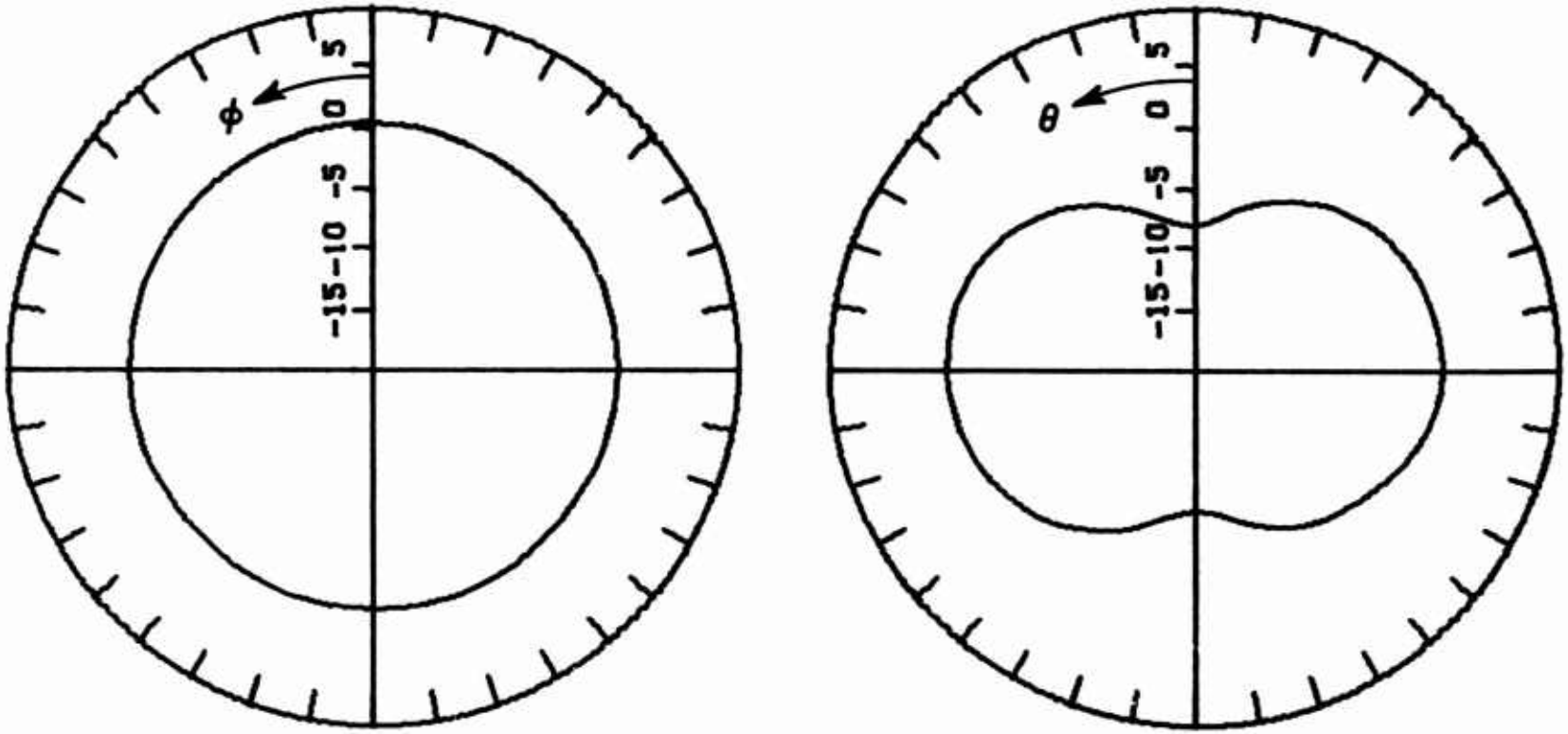

PATTERN IN THE PLANE
THETA = PI/2.

PATTERN IN THE PLANE
PHI = 0.PI.

FREQ. (MHZ) = 500.0
TIP CONFIGURATION 6 DZ = 0.250 IN.

Fig. 9a. $\hat{\phi}$ polarized directivity for the antenna of Fig. 7 at f = 500 MHz.

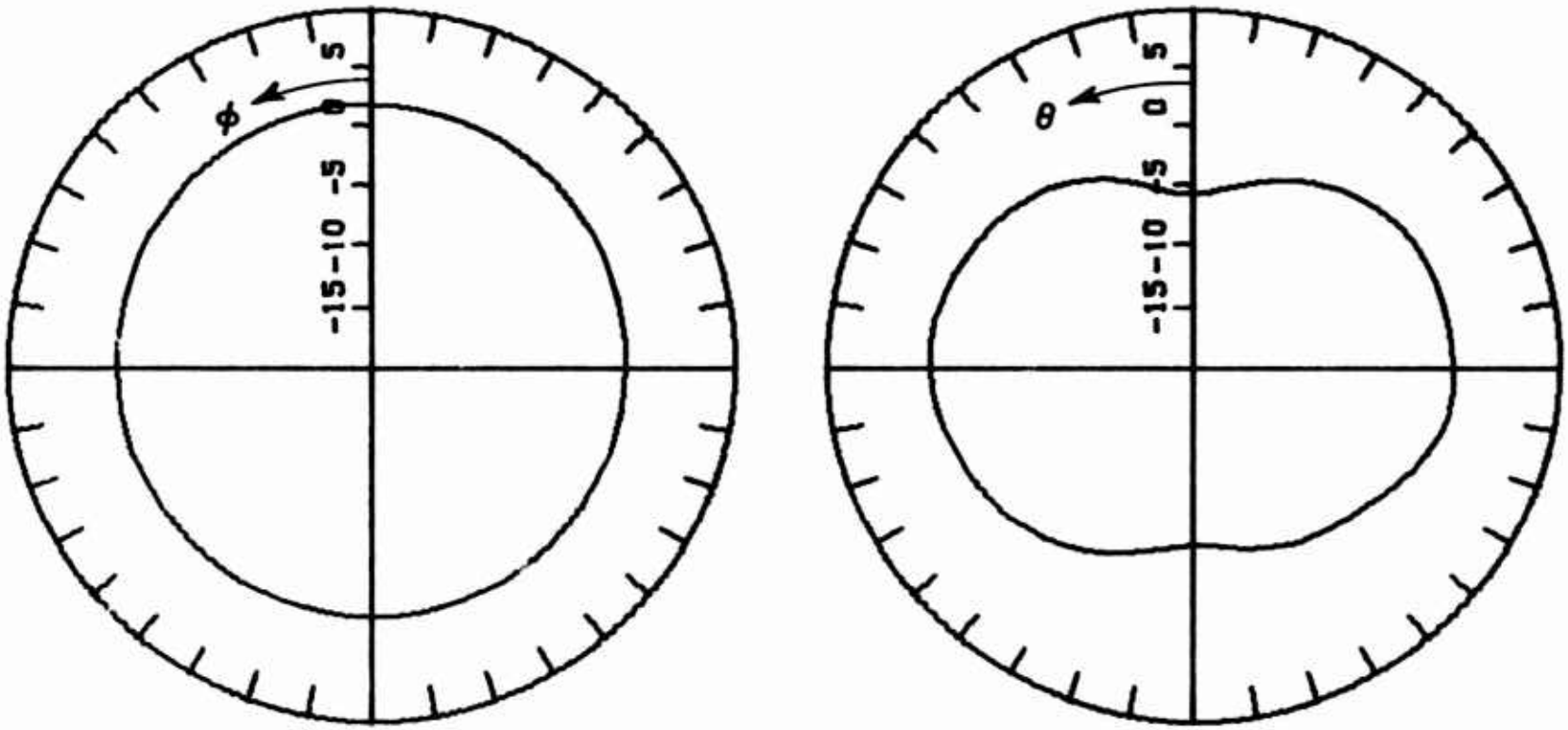

PATTERN IN THE PLANE
THETA = PI/2.

PATTERN IN THE PLANE
PHI = 0.PI.

FREQ. (MHZ) = 600.0
TIP CONFIGURATION 6 DZ = 0.250 IN.

Fig. 9b. $\hat{\phi}$ polarized directivity for the antenna of Fig. 7 at f = 600 MHz.

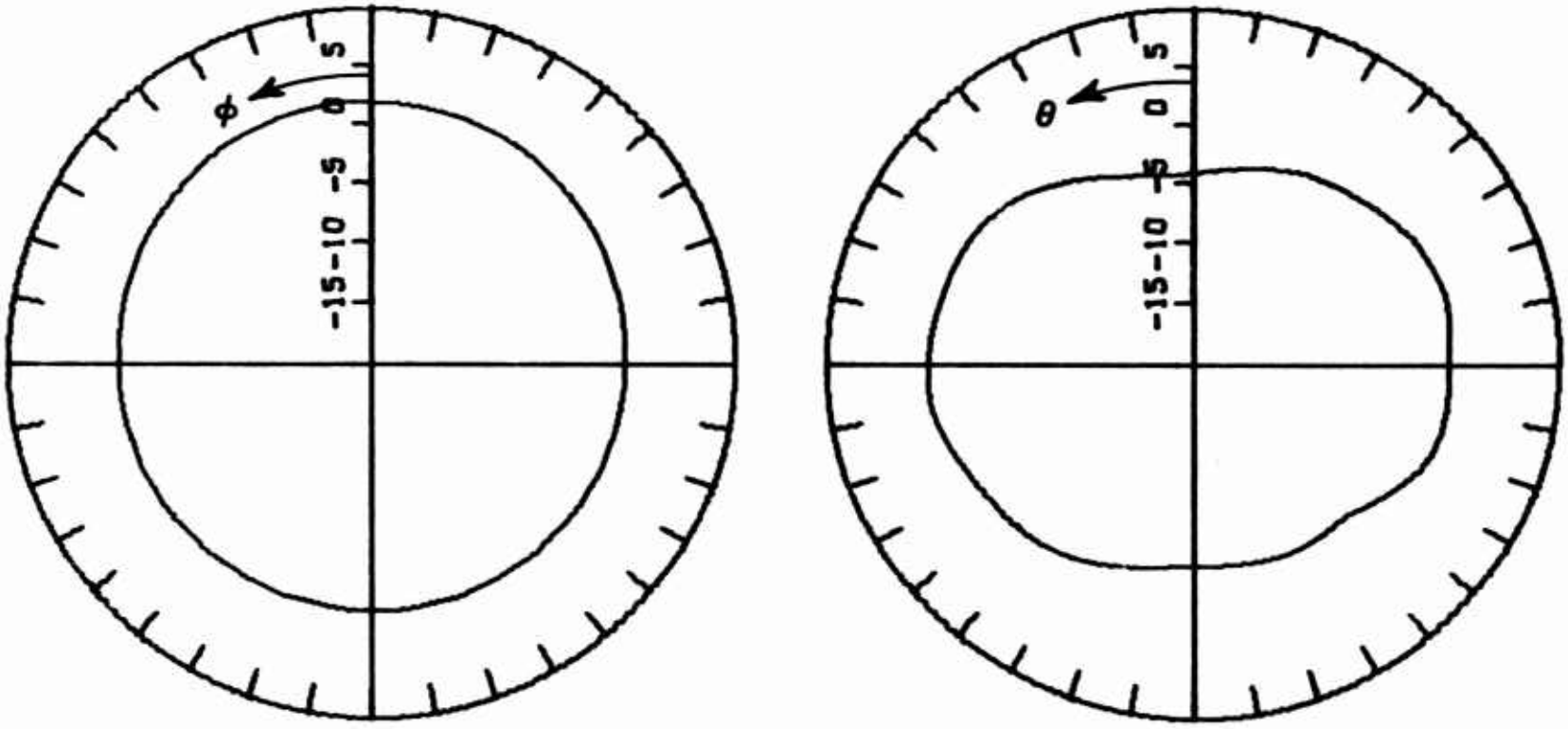

PATTERN IN THE PLANE
THETA = PI/2.

PATTERN IN THE PLANE
PHI = 0.PI.

FREQ. (MHZ) = 700.0
TIP CONFIGURATION 6 DZ = 0.250 IN.

Fig. 9c. $\hat{\phi}$ polarized directivity for the antenna of Fig. 7 at f = 700 MHz.

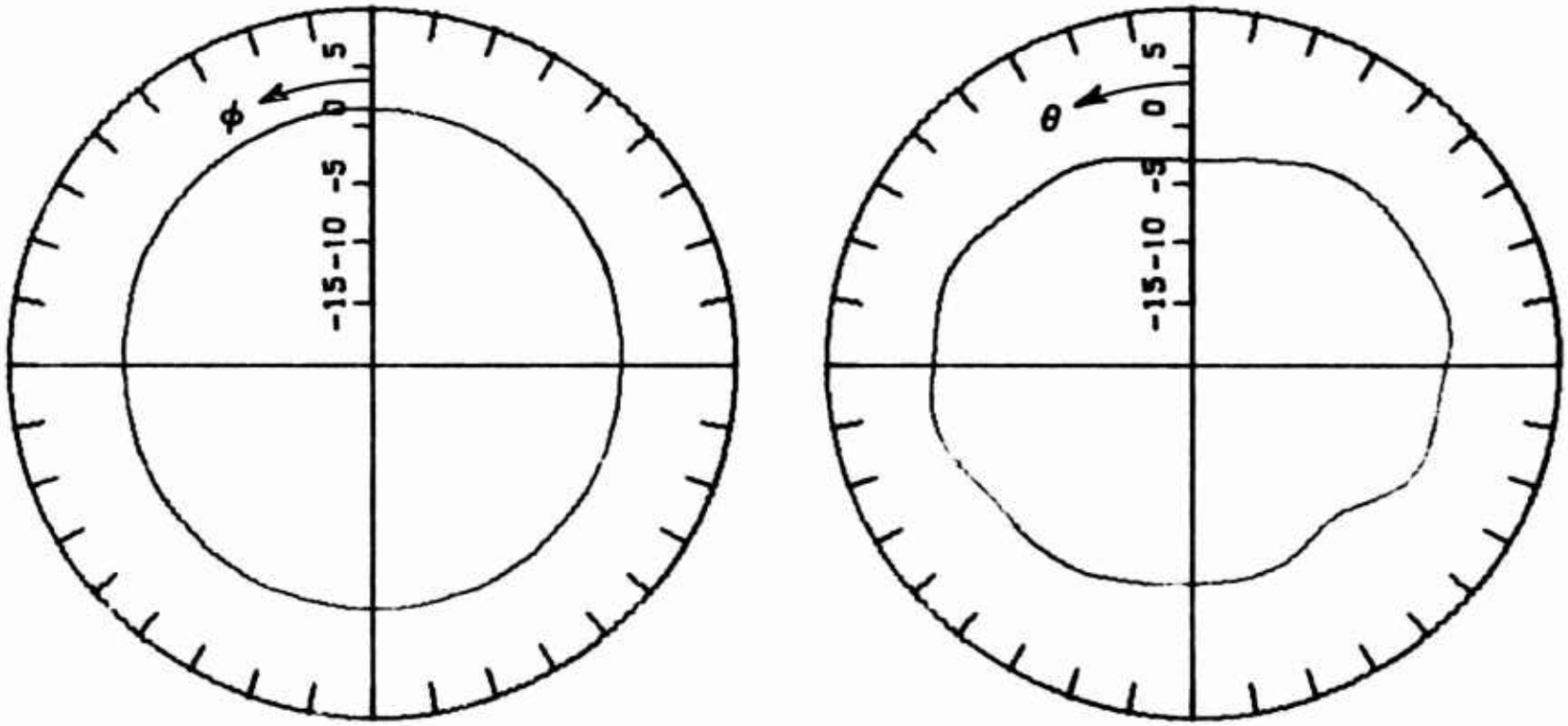

PATTERN IN THE PLANE
THETA = PI/2.

PATTERN IN THE PLANE
PHI = 0.PI.

FREQ. (MHZ) = 800.0
TIP CONFIGURATION 6 DZ = 0.250 IN.

Fig. 9d. $\hat{\phi}$ polarized directivity for the antenna of Fig. 7 at f = 800 MHz.

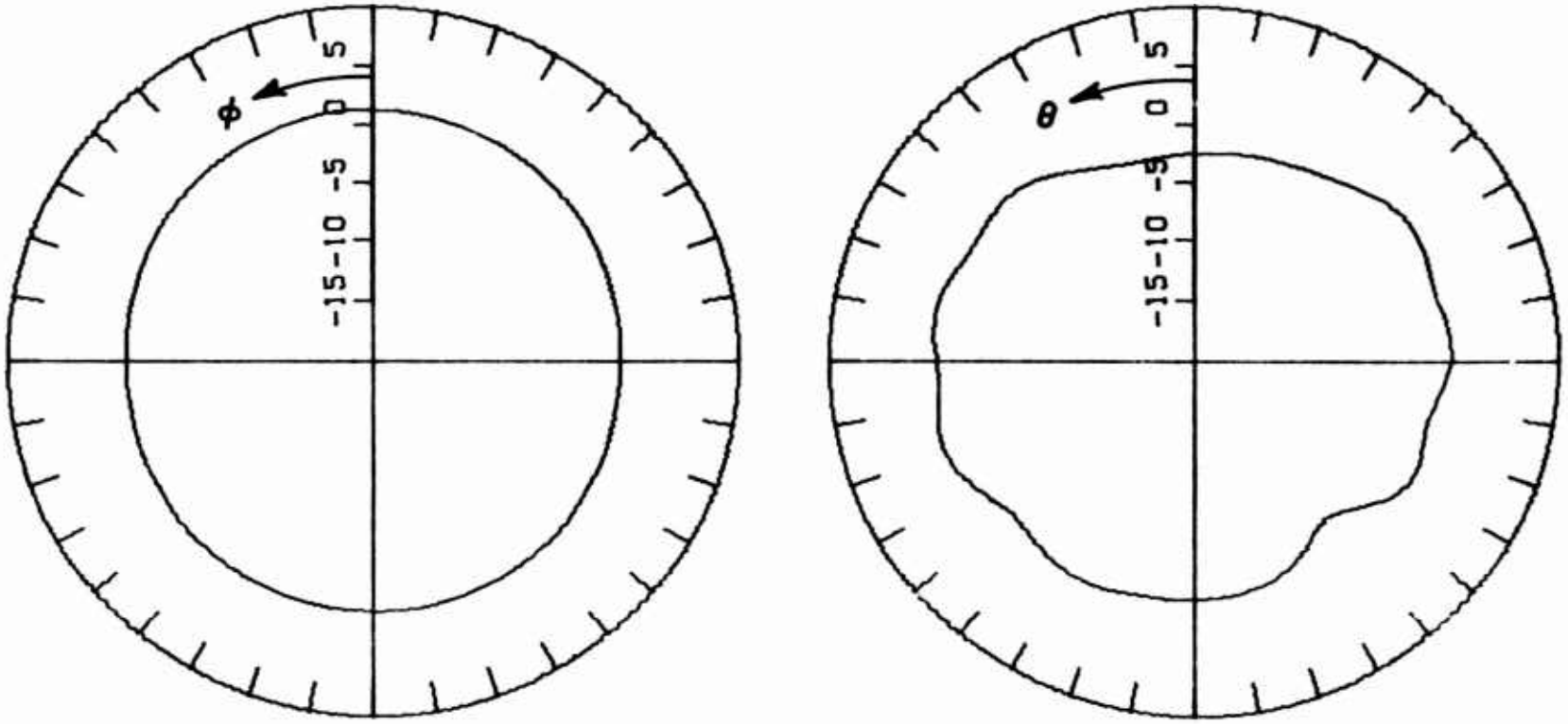

Fig. 9e. $\hat{\phi}$ polarized directivity for the antenna of Fig. 7 at f = 900 MHz.

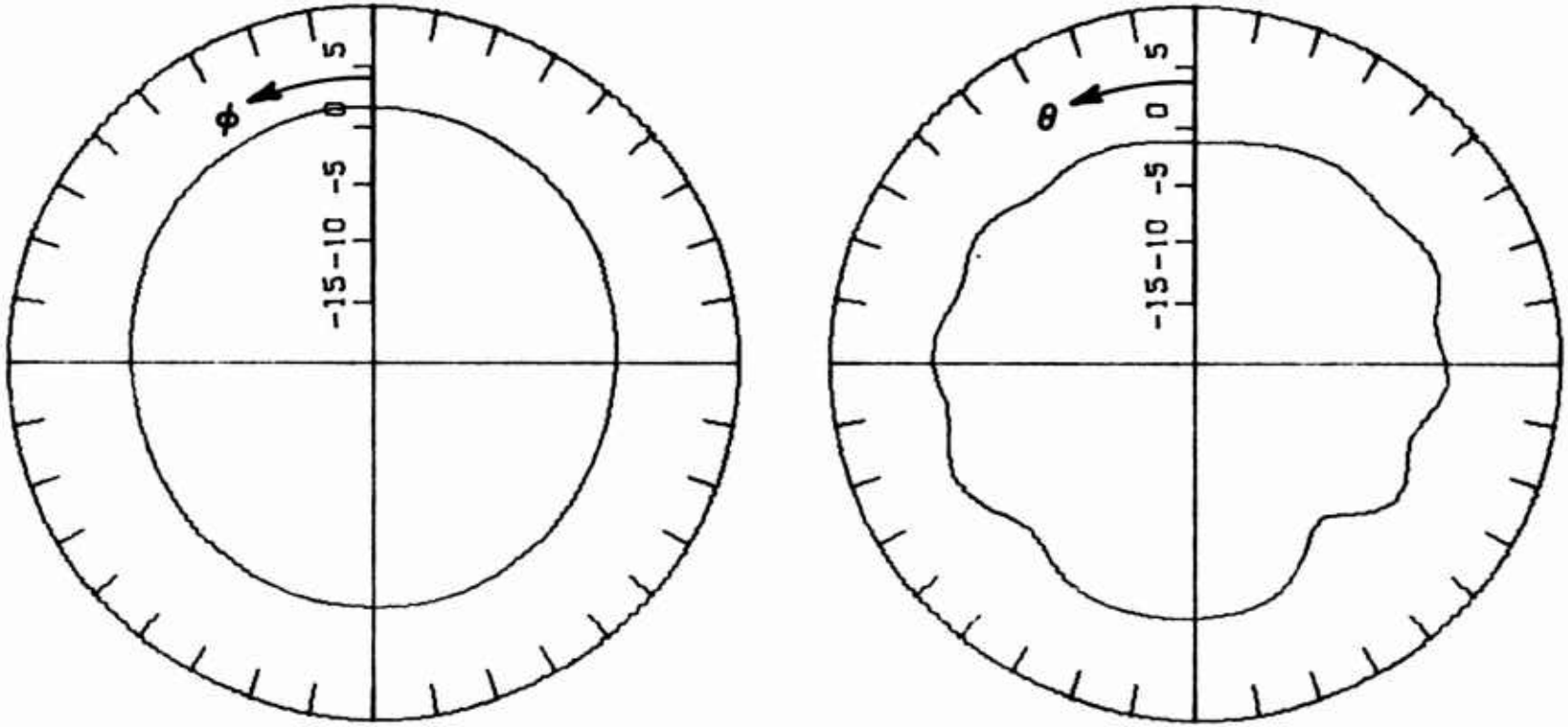

PATTERN IN THE PLANE
THETA = PI/2.

PATTERN IN THE PLANE
PHI = 0,PI.

FREQ. (MHZ) = 1000.0
TIP CONFIGURATION 6 DZ = 0.250 IN.

Fig. 9f. $\hat{\phi}$ polarized directivity for the antenna of Fig. 7 at f = 1000 MHz.

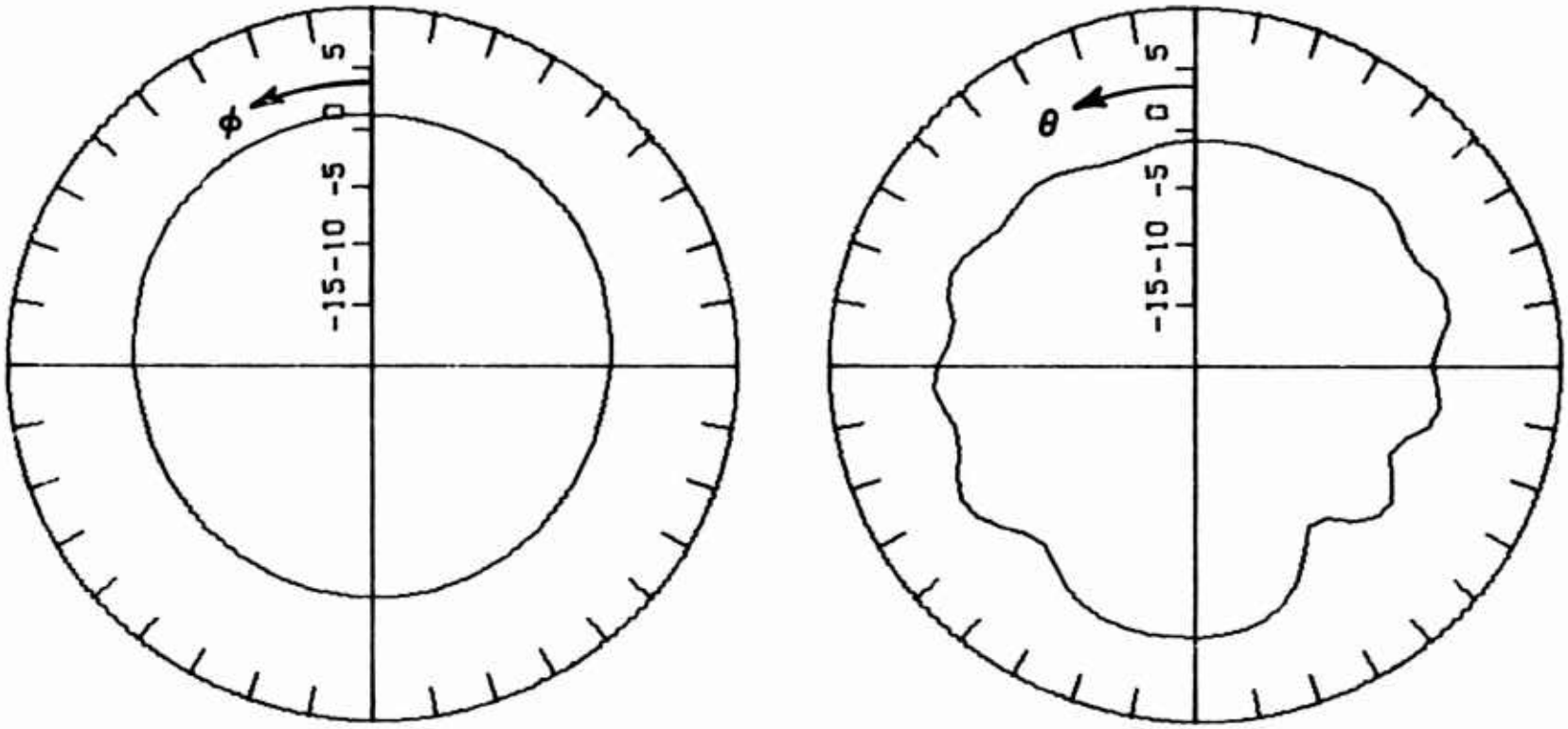

PATTERN IN THE PLANE
THETA = PI/2.

PATTERN IN THE PLANE
PHI = 0.PI.

FREQ. (MHZ) = 1100.0
TIP CONFIGURATION 6 DZ = 0.250 IN.

Fig. 9g. $\hat{\phi}$ polarized directivity for the antenna of Fig. 7 at f = 1100 MHz.

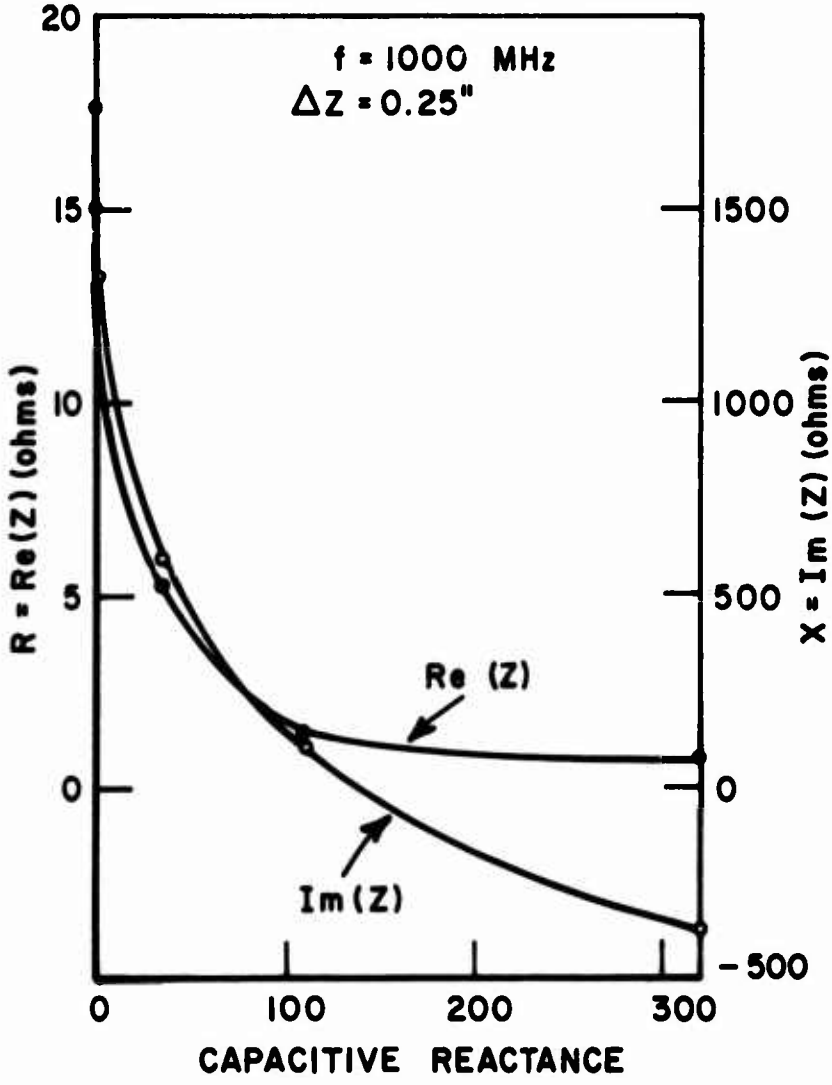

Fig. 10a. The impedance of the antenna of Fig. 7 at f = 1000 MHz plotted versus the reactance of three capacitors inserted in the hexagonal loop.

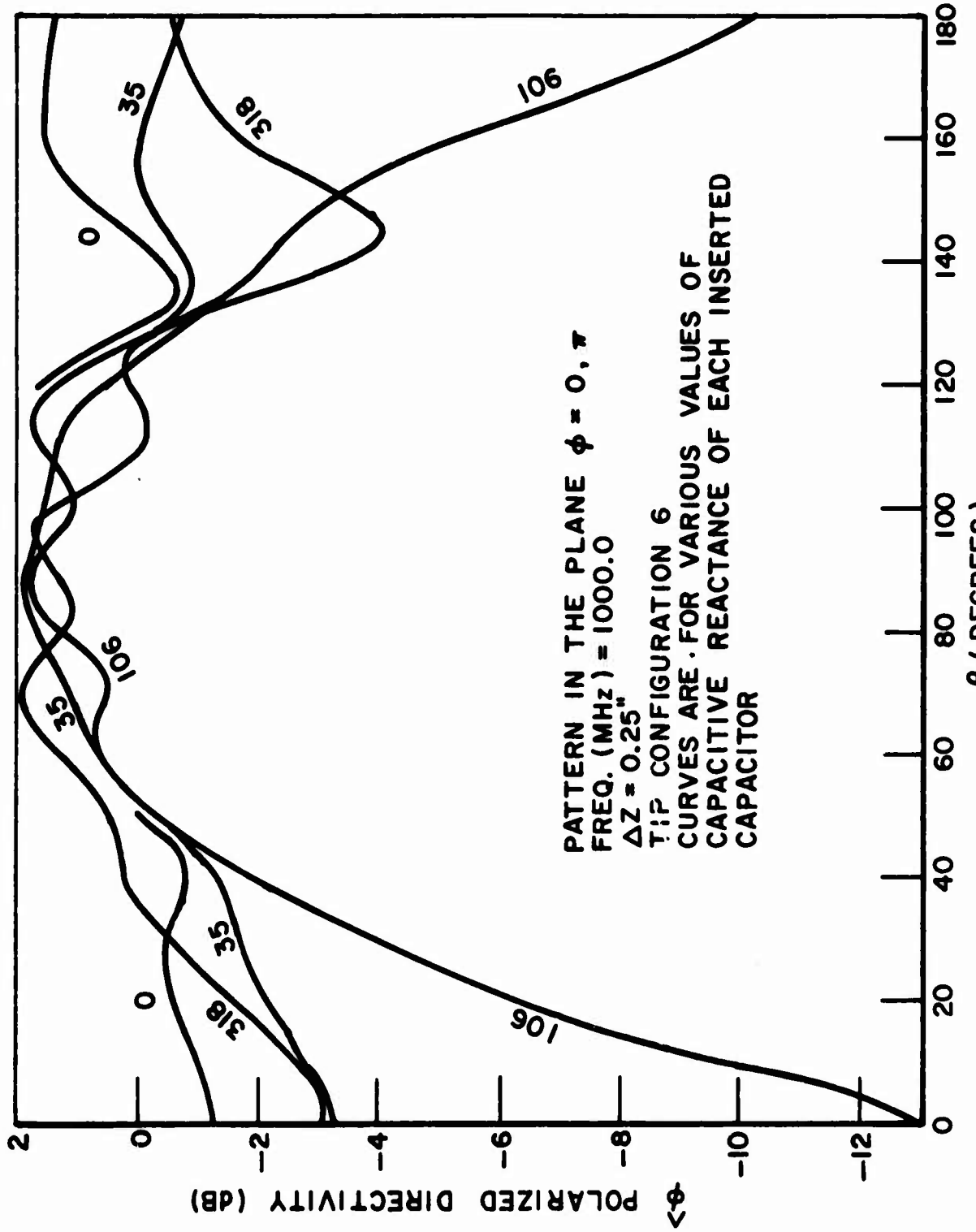

Fig. 10b. The effect of capacitive loading on the patterns in the plane $\phi=0,\pi$ for the antenna shown in Fig. 7. Note that only part of the unloaded curve (0) is shown since it is also shown in Fig. 9f.

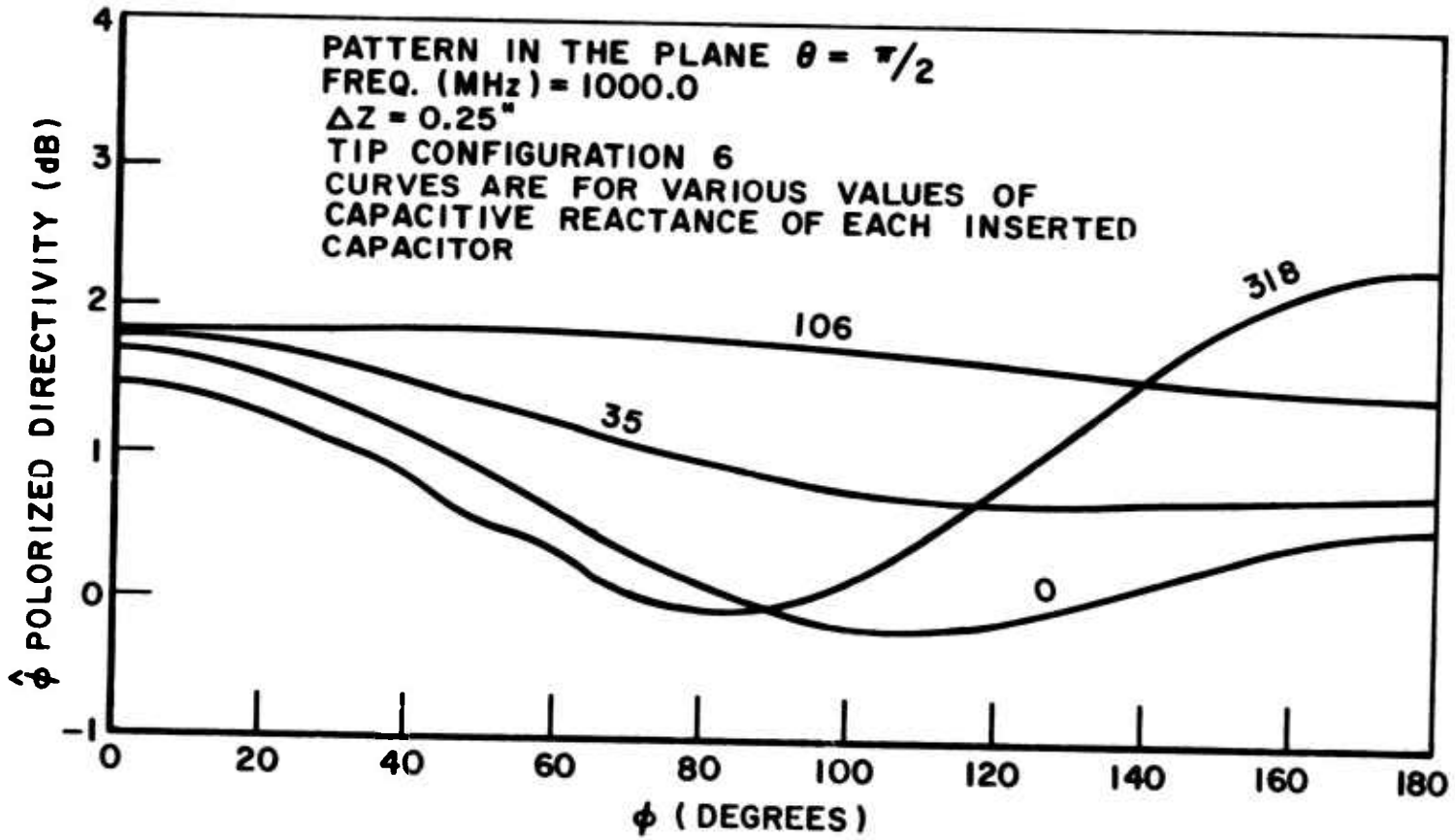

Fig. 10c The effect of capacitive loading on the patterns in the plane $\theta=\pi/2$ for the antenna shown in Fig. 7.

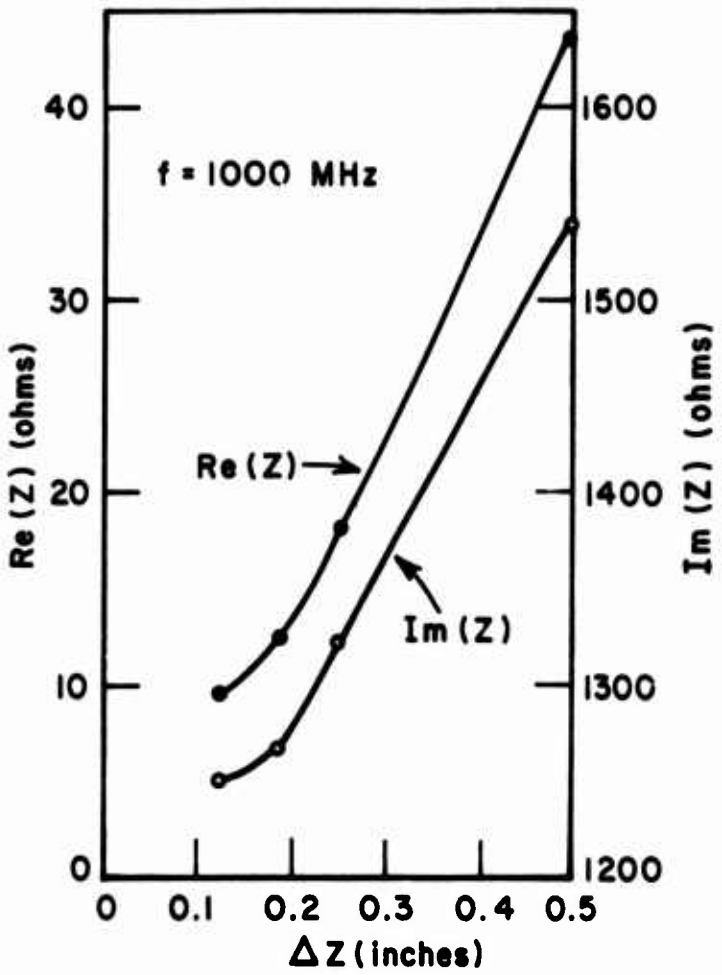

Fig. 11. The impedance of the antenna of Fig. 7 at f = 1000 MHz plotted versus ΔZ.

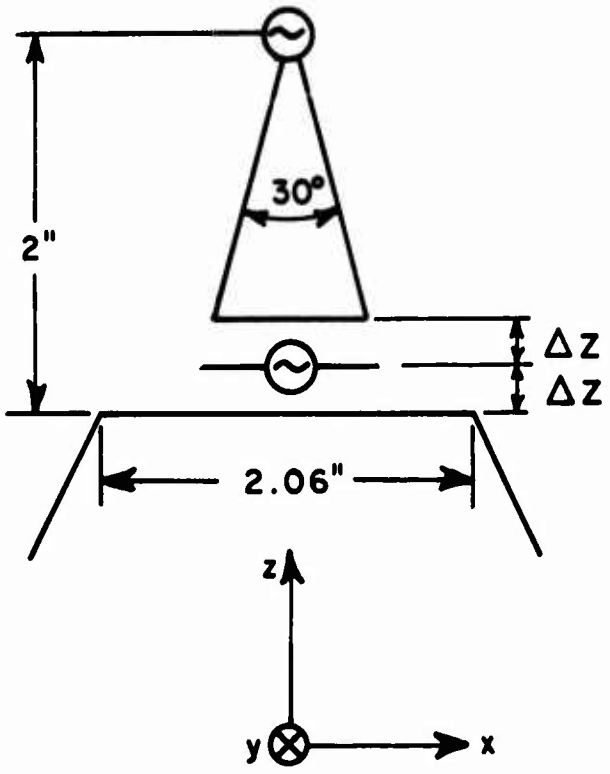

Fig. 12. A loop dipole combination in the tip region of the projectile of Fig. 1.

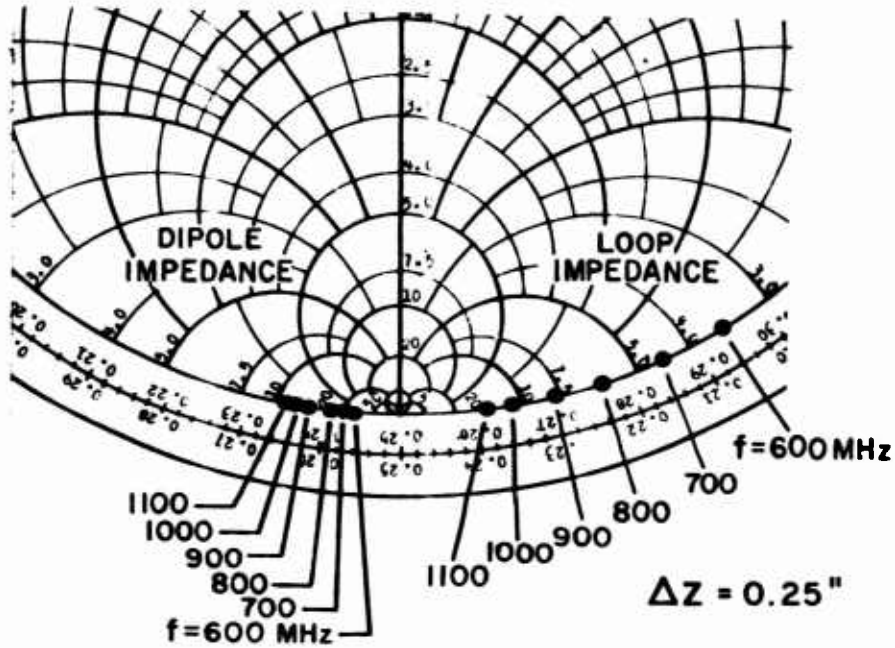

Fig. 13. A Smith Chart plot of the impedance of the antenna of Fig. 12.

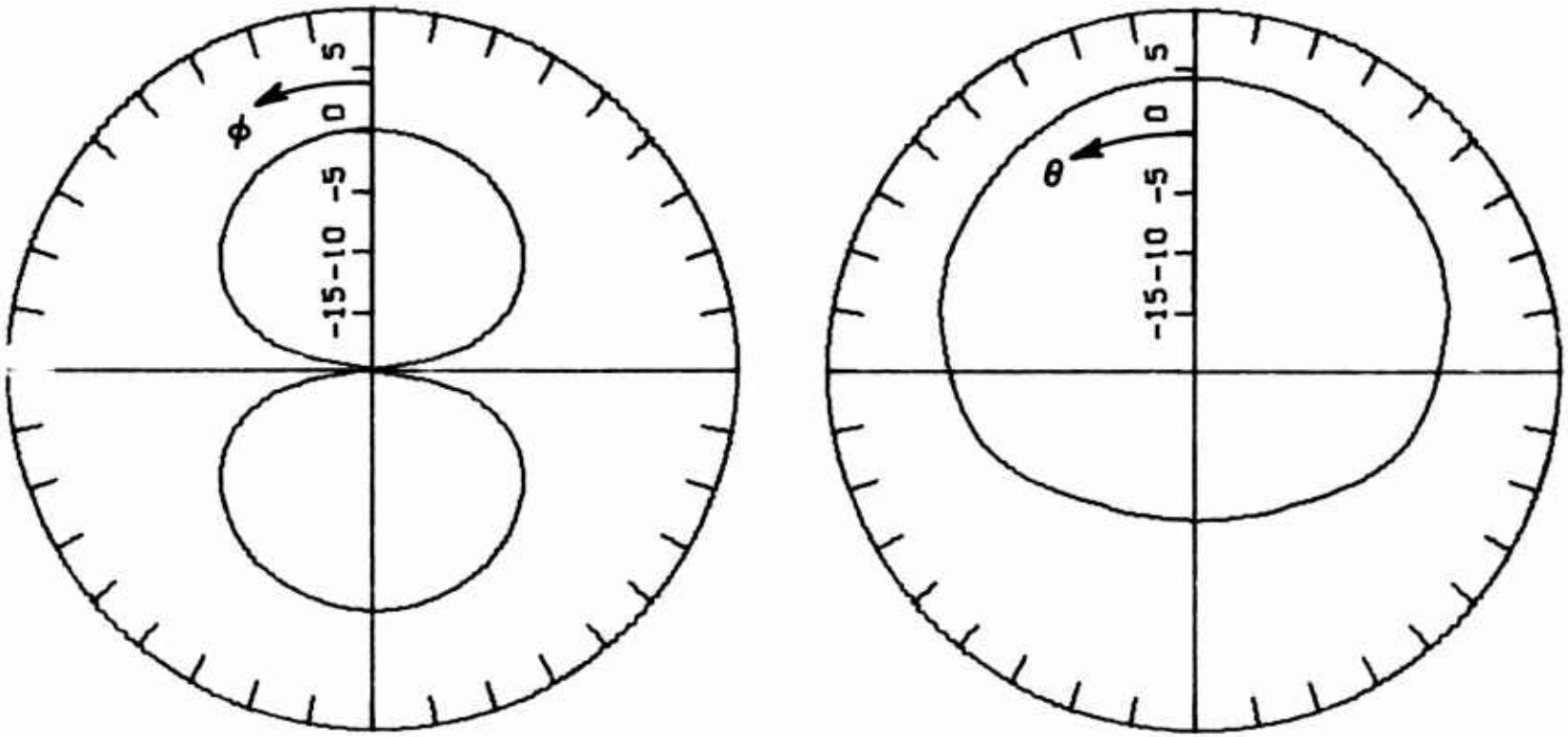

PATTERN IN THE PLANE
THETA = PI/2.

PATTERN IN THE PLANE
PHI = 0.PI.

FREQ. (MHZ) = 600.0
TIP CONFIGURATION 7 DZ = 0.250 IN.

Fig. 14a. $\hat{\theta}$ polarized directivity for the antenna of Fig. 12, V_L = 1.0, V_D = 5.82 + j8.67, and f = 600 MHz.

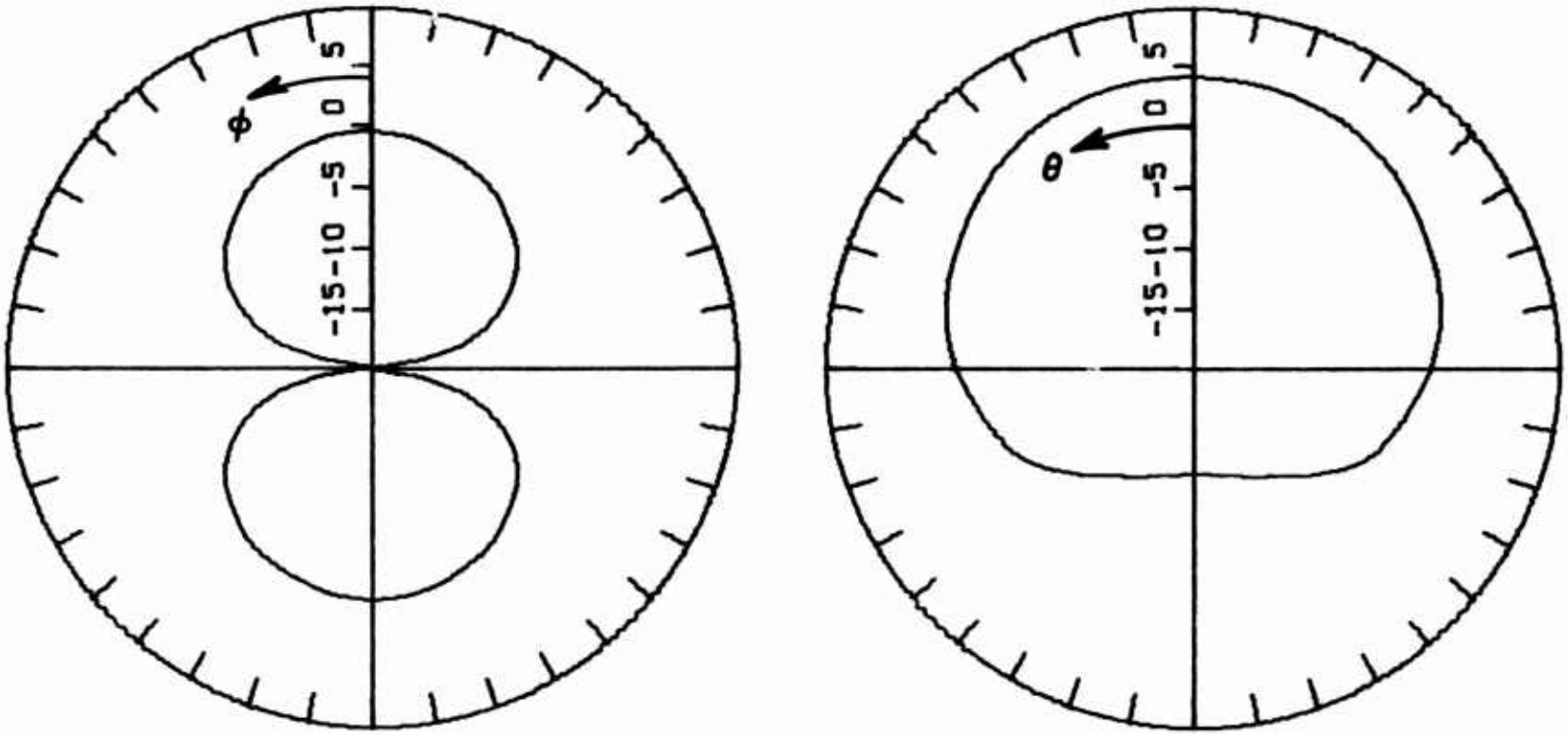

PATTERN IN THE PLANE
THETA = PI/2.

PATTERN IN THE PLANE
PHI = 0.PI.

FREQ. (MHZ) = 700.0
TIP CONFIGURATION 7 DZ = 0.250 IN.

Fig. 14b. $\hat{\theta}$ polarized directivity for the antenna of Fig. 12, V_L = 1.0, V_D = 5.82 + j8.67, and f = 700 MHz.

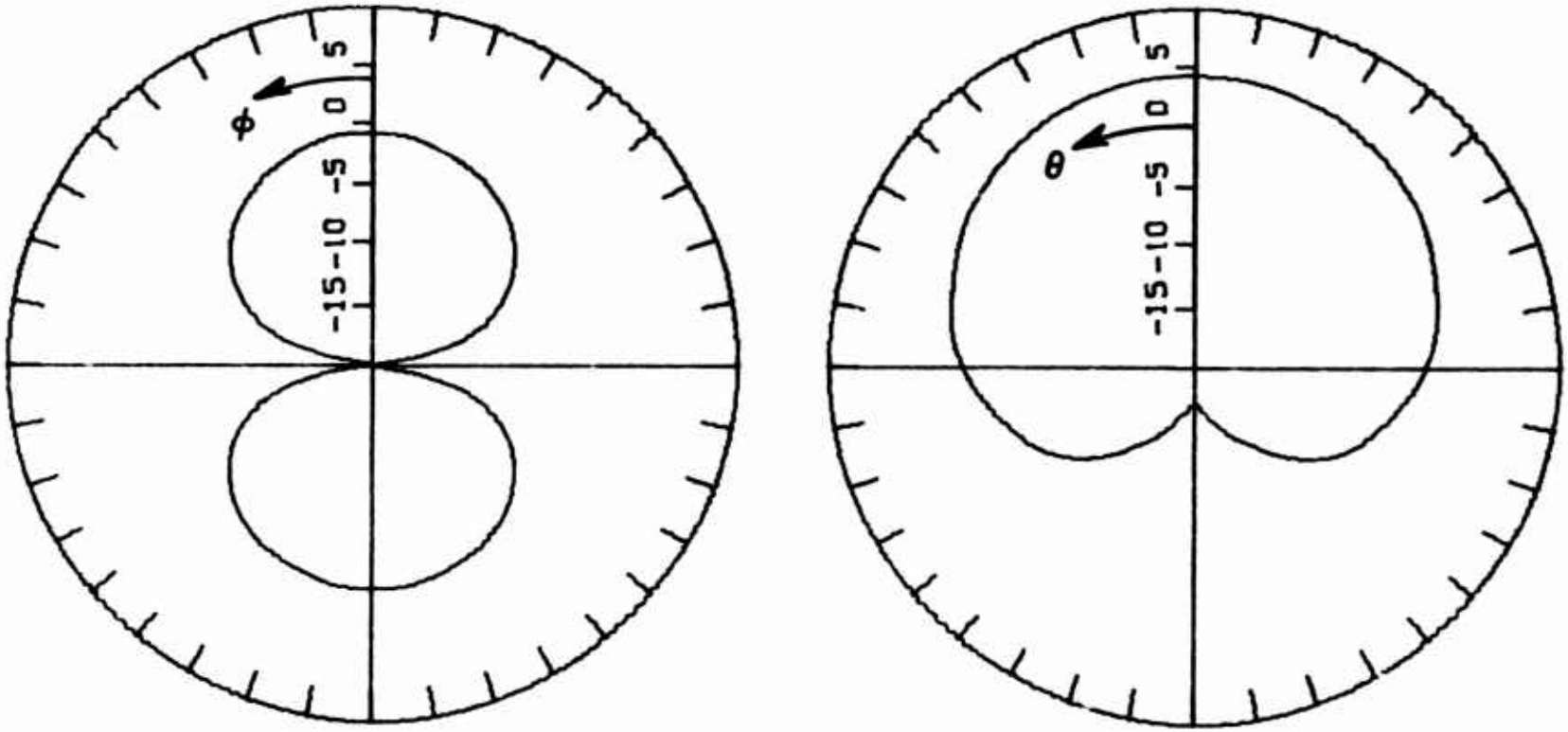

PATTERN IN THE PLANE
THETA = PI/2.

PATTERN IN THE PLANE
PHI = 0.PI.

FREQ. (MHZ) = 800.0
TIP CONFIGURATION 7 DZ = 0.250 IN.

Fig. 14c. $\hat{\theta}$ polarized directivity for the antenna of Fig. 12, $V_L = 1.0$, $V_D = 5.82 + j8.67$, and f = 800 MHz.

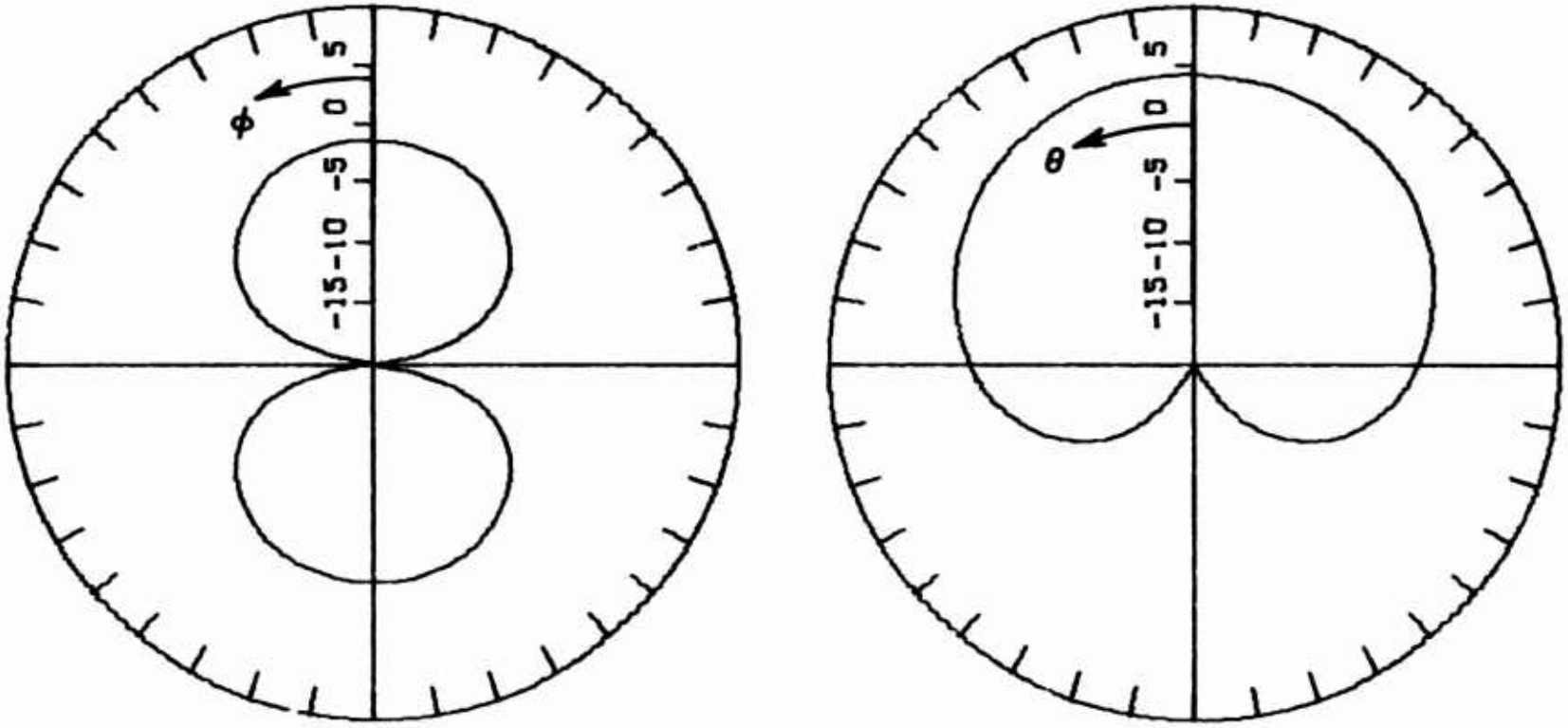

Fig. 14d. $\hat{\theta}$ polarized directivity for the antenna of Fig. 12, V_L = 1.0, V_D = 5.82 + j8.67, and f = 900 MHz.

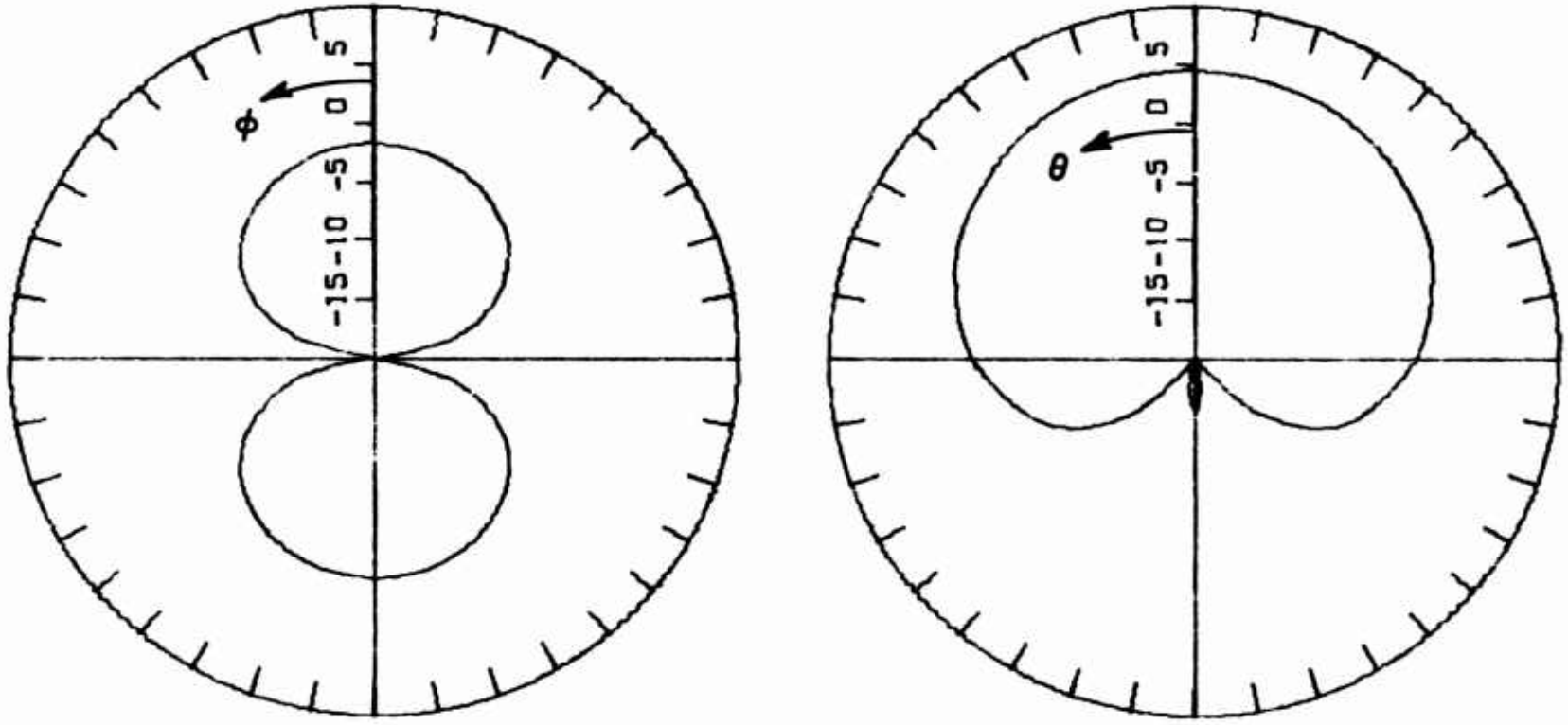

PATTERN IN THE PLANE
THETA = PI/2.

PATTERN IN THE PLANE
PHI = 0.PI.

FREQ. (MHZ) = 1000.0
TIP CONFIGURATION 7 DZ = 0.250 IN.

Fig. 14e. $\hat{\theta}$ polarized directivity for the antenna of Fig. 12, V_L = 1.0, V_D = 5.82 + j8.67, and f = 1000 MHz.

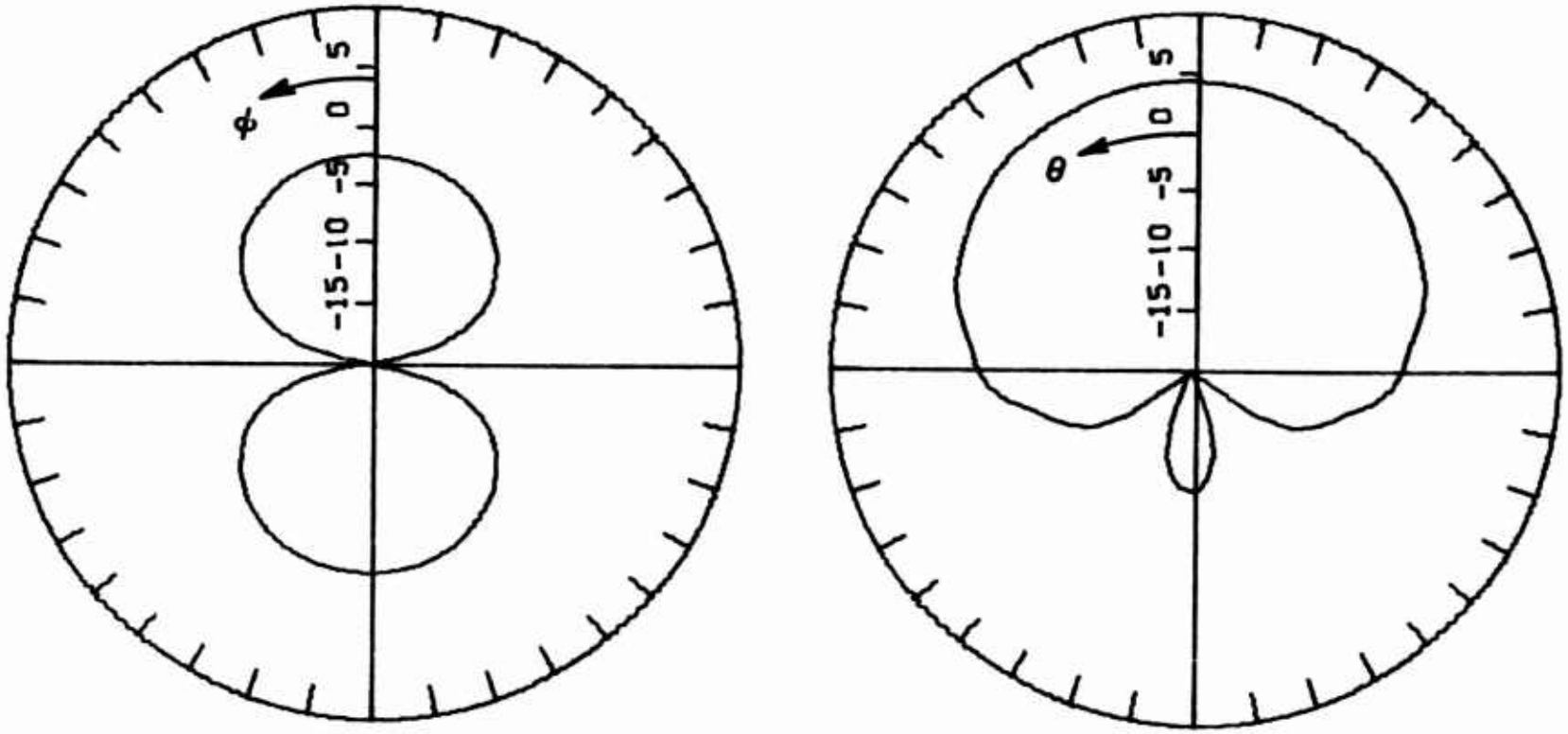

PATTERN IN THE PLANE
THETA = PI/2.

PATTERN IN THE PLANE
PHI = 0.PI.

FREQ. (MHZ) = 1100.0
TIP CONFIGURATION 7 DZ = 0.250 IN.

Fig. 14f. $\hat{\theta}$ polarized directivity for the antenna of Fig. 12, V_L = 1.0, V_D = 5.82 + j8.67, and f = 1100 MHz.

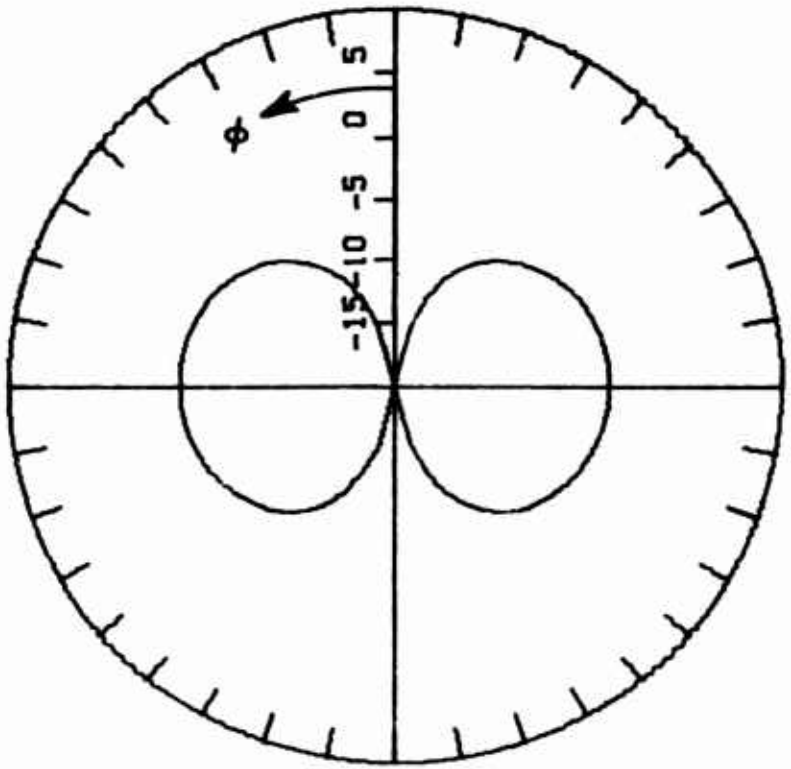

PATTERN IN THE PLANE
THETA = PI/2.
FREQ. (MHZ) = 600.0
TIP CONFIGURATION 7

Fig. 15a. $\hat{\phi}$ polarized directivity for the antenna of Fig. 12, $V_L = 1.0$, $V_D = 5.82 + j8.67$, and f = 600 MHz.

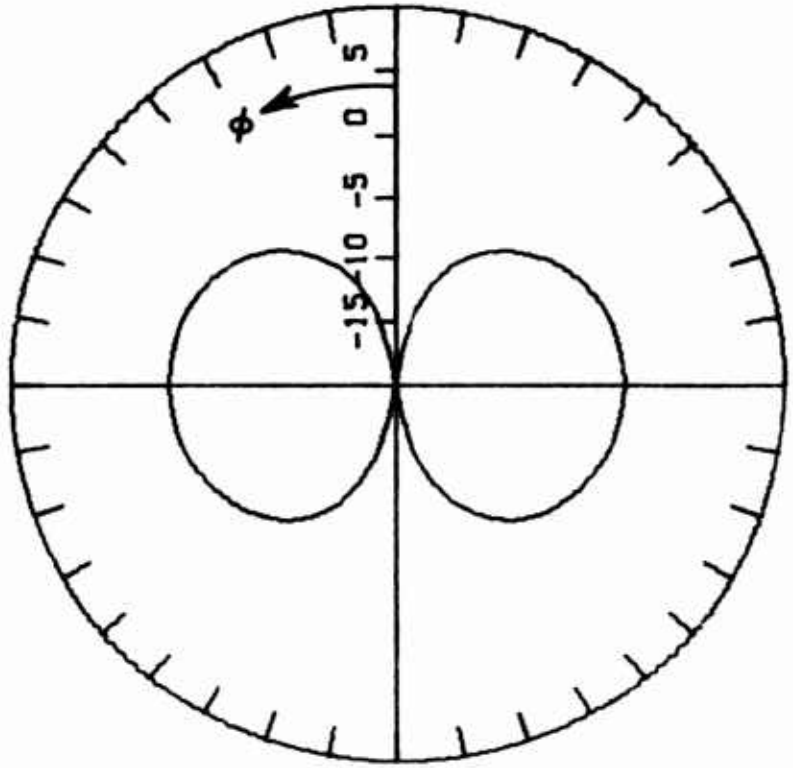

PATTERN IN THE PLANE
THETA = PI/2.
FREQ. (MHZ) = 700.0
DZ = 0.250 IN.

Fig. 15b. $\hat{\phi}$ polarized directivity for the antenna of Fig. 12, $V_L = 1.0$, $V_D = 5.82 + j8.67$, and f = 700 MHz.

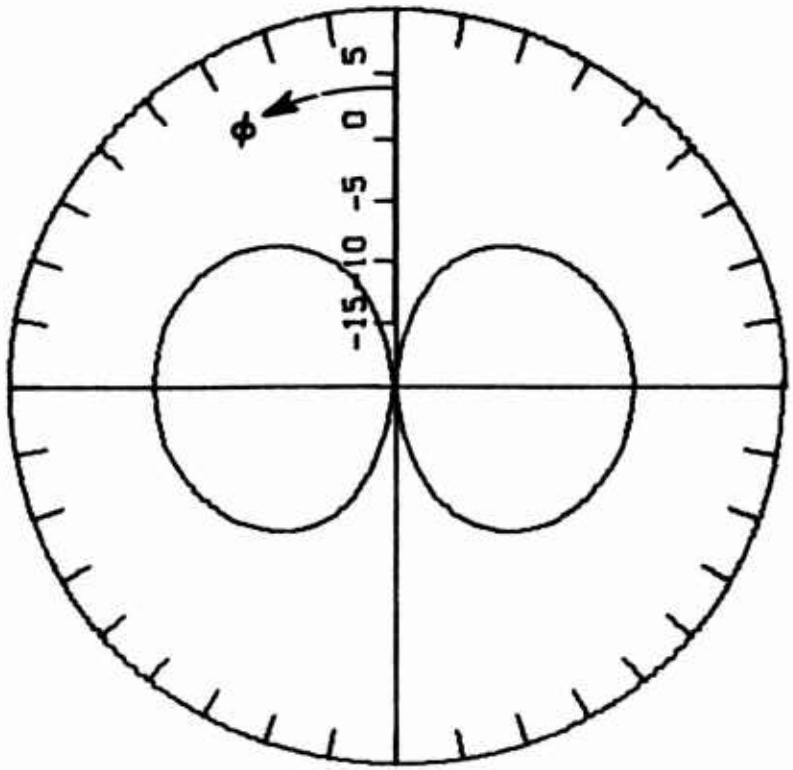

PATTERN IN THE PLANE
THETA = PI/2.
FREQ. (MHZ) = 800.0

Fig. 15c. $\hat{\phi}$ polarized directivity for the antenna of Fig. 12, V_L = 1.0, V_D = 5.82 + j8.67, and f = 800 MHz.

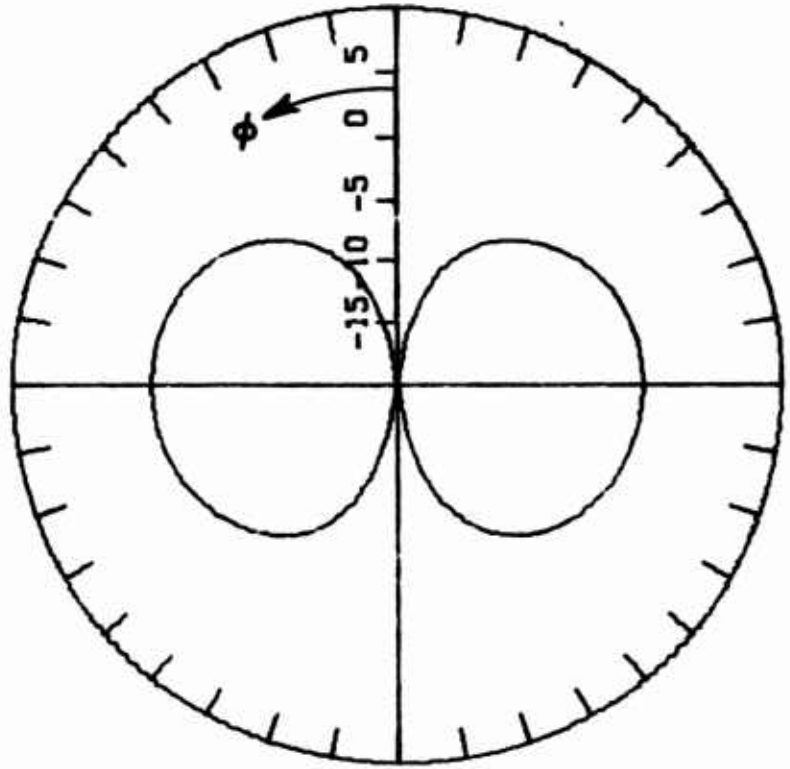

PATTERN IN THE PLANE
THETA = PI/2.
FREQ. (MHZ) = 900.0

Fig. 15d. $\hat{\phi}$ polarized directivity for the antenna of Fig. 12, V_L = 1.0, V_D = 5.82 + j8.67, and f = 900 MHz.

TIP CONFIGURATION 7 DZ = 0.250 IN.

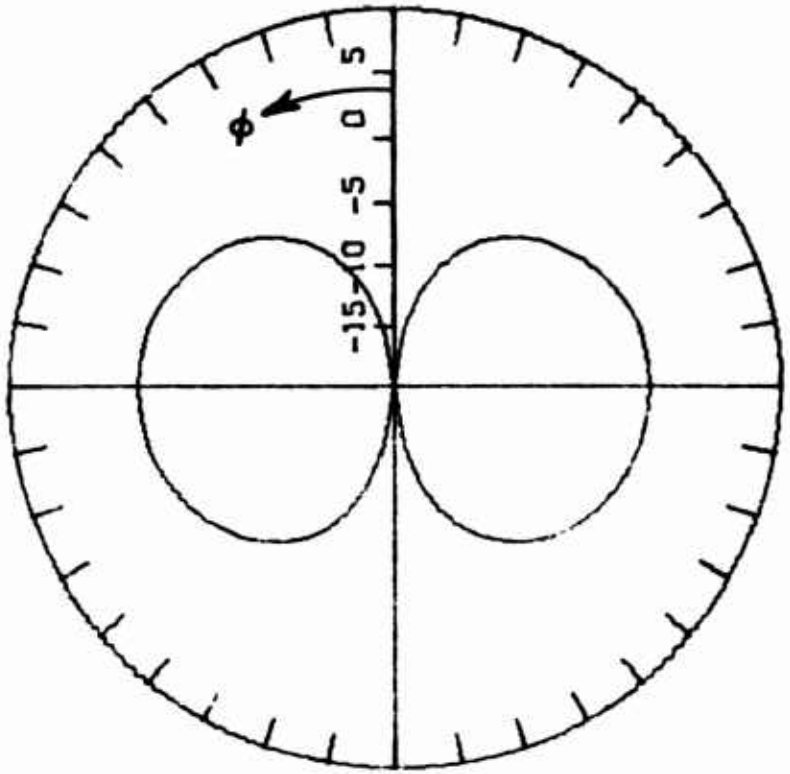

PATTERN IN THE PLANE
THETA = PI/2.
FREQ. (MHZ) = 1000.0

Fig. 15e. $\hat{\phi}$ polarized directivity for the antenna of Fig. 12, $V_L = 1.0$, $V_D = 5.82 + j8.67$, and f = 1000 MHz

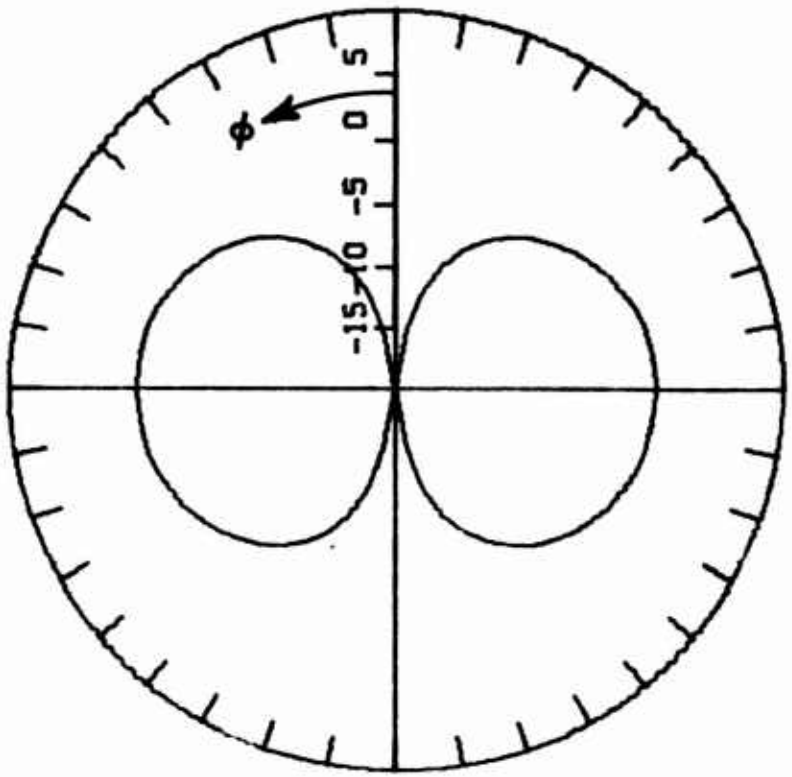

PATTERN IN THE PLANE
THETA = PI/2.
FREQ. (MHZ) = 1100.0

Fig. 15f. $\hat{\phi}$ polarized directivity for the antenna of Fig. 12, $V_L = 1.0$, $V_D = 5.82 + j8.67$, and f = 1100 MHz.

TIP CONFIGURATION 7 DZ = 0.250 IN.

IV. CONCLUSIONS AND RECOMMENDATIONS

The general conclusion that can be made as a result of the study on Contract Number DAAG39-72-C-0041 is that useful design data for projectile-tip antennas can be obtained by computer modelling of the antenna and the projectile body. A computer program using the Method of Moments with piecewise sinusoidal basis functions and utilizing a wire grid representation of the antenna and projectile has been developed and supplied to the sponsor. The details of the program are given in the references cited in this report.

The computer model uses round wire segments and will give very good results when the antenna (in the tip of the projectile) is made of round wires. If the actual antenna is composed of wire segments of other than circular cross-section, the non-circular wires should be replaced by equivalent circular wires.[8] A perfectly conducting strip of width 2w is equivalent to a perfectly conducting round wire of diameter w.

If the antenna is embedded in or etched on a dielectric substrate, or enclosed by a dielectric cover (radome), the present model will be somewhat in error but will still give guideline results. As part of the study on this contract, the problem of a conducting strip dipole in or on a dielectric slab was formulated and agreement between calculated and measured results shows that the formulation is valid and that the dielectric material can cause a noticeable reduction in the resonant frequency, the factor being always less than the square root of the dielectric constant.

Since many practical antennas for missile and projectile applications involve dielectric substrates and/or radome covers, it is recommended that the formulation developed on this program be extended and applied to an arbitrary conducting strip configuration on a dielectric substrate and enclosed by a small radome. This should include also the difficult problem of the proximity effect wherein the current distribution over the width of the strip is altered by the proximity of another current carrying strip. Antenna efficiency is influenced greatly by the current distribution as is the impedance but to a lesser extent.

The extension of the analysis of conducting strip antennas in or on dielectric substrate also would provide a design tool for so-called microstrip antennas. These consist of etched conducting configurations on dielectric substrate bonded to a metal surface such as the body of a missile or projectile. Such elements generally have resonant lengths of conducting strips but the structure is very thin electrically. Microstrip antennas look very promising as low profile or flush mounted antennas for upper UHF and VHF. At present there is no general design procedure or useful body of design data for such antennas.

---

[8] R.W.P. King, The Theory of Linear Antennas, Harvard University Press, Cambridge, Mass., (1956), pp. 16-20.

V. LITERATURE CITED

1 R. F. Harrington, "Field Computation by Moment Methods," Macmillan, 1968.

2 J. H. Richmond, "Radiation and Scattering by Thin-Wire Structures in the Complex Frequency Domain," Report 2902-10, July 1973, The Ohio State University ElectroScience Laboratory, Department of Electrical Engineering; prepared under Grant No. NGL 36-008-138 for National Aeronautics and Space Administration.

3 "Computer Techniques for Electromagnetics," vol. 7, edited by R. Mittra, Pergamon Press, 1973, Chapter 2.

4 J. H. Richmond, "Computer Program for Thin-Wire Structures in a Homogeneous Conducting Medium," Report 2902-12, August 1973, The Ohio State University ElectroScience Laboratory, Department of Electrical Engineering; prepared under Grant No. NGL 36-008-138 for National Aeronautics and Space Administration.

5 J. H. Richmond, "Computer Analysis of Three-Dimensional Wire Antennas," Report 2708-4, December 1969, The Ohio State University ElectroScience Laboratory, Department of Electrical Engineering; prepared under Contract DAAD05-69-0031 for Aberdeen Proving Ground.

6 C. H. Walter and E. H. Newman, "Electrically Small Antennas," Report 3281-3, February 1974, The Ohio Sttate University ElectroScience Laboratory, Department of Electrical Engineering; prepared under Contract DAAG 39-72-C-0041 for Department of the Army, Harry Diamond Laboratories.

7 E. H. Newman, "Strip Antennas in or on an Electrically Thin Dielectric Slab," Report 3281-4 (in preparation), The Ohio State University ElectroScience Laboratory, Department of Electrical Engineering; prepared under Contract DAAG 39-72-C-0041 for Department of the Army, Harry Diamond Laboratories.

8 R. W. P. King, The Theory of Linear Antennas, Harvard University Press, Cambridge, Mass., (1956), pp. 16-20.